NATIONAL ADVISORY COMMITTEE
FOR AERONAUTICS

TECHNICAL NOTE 2066

CORRELATION OF EFFECTS OF FUEL-AIR RATIO, COMPRESSION

RATIO, AND INLET-AIR TEMPERATURE ON KNOCK LIMITS

OF AVIATION FUELS

By Leonard K. Tower and Henry E. Alquist

Lewis Flight Propulsion Laboratory
Cleveland, Ohio

NACA

NATIONAL ADVISORY COMMITTEE FOR AERONAUTICS

TECHNICAL NOTE 2066

CORRELATION OF EFFECTS OF FUEL-AIR RATIO,

COMPRESSION RATIO, AND INLET-AIR TEMPERATURE ON

KNOCK LIMITS OF AVIATION FUELS

By Leonard K. Tower and Henry E. Alquist

SUMMARY

A method of relating the effects of fuel-air ratio on the knock-limited charge flow and power of a supercharged engine with those of compression ratio and inlet-air temperature is presented. These variables are correlated by means of a relation between knock-limited end-gas density and end-gas temperature calculated from engine-inlet conditions at incipient knock. Knock data obtained in a CFR engine over a wide range of conditions were correlated for the following eight fuels: 28-R fuel, aviation alkylate, S reference fuel, diisopropyl, triptane, cyclohexane, cyclopentane, and triptene. Charts are also presented by means of which knock-limited charge flow and indicated mean effective pressure may be determined for a fuel when its correlation curve is known.

When knock-limited charge flow calculated from the correlation curves was compared with experimentally determined charge flow for each fuel over many conditions, the smallest mean error was 2.7 percent for 28-R fuel and the largest mean error was 8.6 percent for triptane. The mean error in calculated charge flow for all the fuels at all the operating conditions investigated was 5.0 percent.

INTRODUCTION

The complete evaluation of the knock-limited performance of a fuel in a spark-ignition engine requires knowledge of the effects of many variables such as fuel-air ratio, compression ratio, inlet-air temperature, spark advance, and engine speed. If a correlation could be obtained among some of these variables, the amount of data required for a comprehensive evaluation of performance would be greatly reduced. The knock-limited performance could be predicted over a considerable range of operating conditions from a limited amount of engine data.

In references 1 and 2, it is shown that knock-limited performance data for changes in compression ratio and inlet-air temperature can be correlated by means of knock-limited end-gas density and end-gas temperature. The end-gas conditions for the data of reference 1 were calculated from the ideal gas laws using inlet-air pressure, inlet-air temperature, and compression ratio. The end-gas density and temperature of reference 2 were calculated by using the cylinder gas pressure shortly after the start of compression, the cylinder gas pressure just prior to knock (as measured by an engine indicator), the cylinder volumes at these points in the cycle, and the quantity of air, fuel, and residuals present in the cylinder. Other variables such as fuel-air ratio were not, however, correlated with compression ratio or inlet-air temperature by the methods presented in reference 1 and reference 2.

A satisfactory and simpler method of correlating the effects of compression ratio and inlet-air temperature on the knock-limited performance of a fuel in an engine is described in reference 3. The knock-limited compression-air density is plotted against the compression-air temperature calculated by adiabatic-compression formulas from the intake conditions. Once the correlation has been obtained for a given fuel in an engine, the knock-limited indicated mean effective pressure of the same fuel in the same engine at any condition of inlet-air temperature and compression ratio can readily be determined. Furthermore, data at only a few compression ratios or inlet-air temperatures are needed to establish the correlation. Inasmuch as fuel-air ratio was not included in the correlation, a separate correlation was necessary for each fuel-air ratio. Spark advance and engine speed were not varied in this investigation.

An investigation was conducted at the NACA Lewis laboratory to determine if the effects of fuel-air ratio on the knock-limited charge flow of a supercharged engine could be included in a correlation with those of compression ratio and inlet-air temperature, thereby reducing the data required to evaluate the performance of a fuel. Data for eight fuels obtained on a CFR engine and covering a wide range of fuel-air ratios, compression ratios, and inlet-air temperatures are used to establish such a correlation. A single relation for each fuel is made between knock-limited end-gas density and end-gas temperature, calculated from inlet conditions, for variations in fuel-air ratio, compression ratio, and inlet-air temperature. Variation in fuel-air ratio is assumed to have an effect on cylinder combustion temperature, which is expressed as a function of fuel-air ratio. A method for determining this function of fuel-air ratio for each fuel from engine data is presented.

APPARATUS

Engine. - The principal data presented were obtained with a supercharged CFR engine. The engine was equipped with an aluminum piston, a sodium-cooled exhaust valve, and a cylinder having four holes. In order to improve cyclic reproducibility, a 180° shrouded intake valve was used. A variation of speed of ± 1.3 percent occurred because the dynamometer was not speed-compensated for changes in load. A schematic diagram of the cylinder showing the location of the spark plugs, the knock pickup, and the position of the shroud is presented in figure 1.

Ignition system. - The sparking voltage was supplied to each of two spark plugs by separate spark coils. Spark advance was manually controlled.

Air system. - A schematic diagram of the air system is shown in figure 2. Air at a pressure of 110 pounds per square inch was supplied from the laboratory system to regulator A, which was capable of holding the pressure to within 0.1 inch of mercury of the desired pressure. The rate of air flow was determined by a square-edge orifice D. The static pressure at the orifice was measured by mercury manometer G and the differential pressure at the orifice was measured by a water manometer K. The air temperature was measured by thermocouples C.

The air passed from the measuring orifice to an electric air heater E; the heater current was manually regulated. In addition, the air temperature was controlled by a butterfly valve on the heater intake, which varied the amount of air that was allowed through the heating elements of the heater. From the heater, the air was tangentially directed into a surge tank F, which was attached to the inlet manifold J. The engine inlet-air temperature was measured at the outlet of the surge tank.

The engine exhausted through a 10-foot length of 2-inch pipe into the laboratory exhaust trench. A draft fan held the exhaust-trench pressure about 2 inches of water below atmospheric pressure.

Fuel system. - A schematic diagram of the fuel system is presented in figure 3. An automatic fuel-measuring system was used that weighed out fuel to the engine and recorded the time and the number of engine revolutions during which the fuel was consumed by the engine. The components of this system, shown in figure 3, are the two solenoid valves C and the fuel-weighing stand E, consisting of a balance and a beaker. The system automatically refilled the

beaker after the measured amount of fuel had been supplied to the
engine. For control purposes, the rate of fuel flow was indicated
by rotameter D. After passing through the rotameter, the fuel was
circulated through a single-cylinder high-pressure injection pump H
by a small centrifugal circulating pump K. The fuel pressure
from the centrifugal pump was maintained at 10 pounds per square
inch by the pressure-relief valve G. A fuel cooler J in the cir-
culating system removed heat generated by the injection pump. The
fuel was injected into the intake manifold parallel to the air
stream at a pressure of 1200 pounds per square inch. The time of
injection was 50° B.T.C. on the intake stroke.

Cooling system. - Two types of cooling system were used: an
evaporative system containing a mixture of ethylene glycol and
water or a system using water under pressure as a coolant. In the
pressurized cooling system, a pump circulated the water through the
jacket and the heat exchanger; the desired coolant-outlet tempera-
ture was maintained by an automatic regulator, which controlled the
amount of cooling water to the heat exchanger. In both the evapora-
tive system and the pressurized system, a coolant-outlet temperature
of 250° F was maintained for all runs.

Oil-temperature control. - The oil temperature was maintained
manually at 145° F for all determinations.

Knock detection. - Knock was detected by a cathode-ray oscil-
loscope in conjunction with a magnetostriction internal pickup unit.
The leads from the magnetostriction pickup were connected to a 4000-
to 10,000-cycles-per-second band-pass filter and then to the oscil-
loscope. Thus, only the pressure fluctuations due to gas vibrations
having frequencies in the pass band were visible on the oscilloscope
screen.

Power measurement. - Indicated mean effective pressure was cal-
culated from the sum of the brake and friction horsepowers. Friction
horsepower was approximately determined by motoring the engine
immediately after taking each point.

FUELS

In establishing the correlation among fuel-air ratio, compres-
sion ratio, and inlet-air temperature based on the computation of
end-gas densities and temperatures from the manifold condition, the
following fuels were used:

28-R fuel
Aviation alkylate
S reference fuel
Diisopropyl (2,3-dimethylbutane)
Triptane (2,2,3-trimethylbutane)
Cyclohexane
Cyclopentane
Triptene (2,2,3-trimethyl-1-butene)

All fuels were leaded to 4 ml TEL per gallon except 28-R, specifications for which require 4.6 ml TEL per gallon.

THEORY

In order to correlate the effects of fuel-air ratio, compression ratio, and inlet-air temperature on the knock-limited power, the knock-limited end-gas density and end-gas temperature conditions were employed. A method was devised for computing the end-gas density and end-gas temperature from inlet-air temperature, compression ratio, fuel-air ratio, and knock-limited air-flow data. All these items are usually obtained in the supercharged-engine knock tests.

In the consideration of an ideal cycle for an engine condition at which incipient knock occurs, the cylinder contents, including the portion known as the end gas, are assumed to be compressed adiabatically to top center. The state of the mixture at top center is then described by the compression charge density and compression-air temperature:

$$\rho_c = \frac{W}{V_c} \tag{1}$$

$$T_c = T_o (r)^{\gamma - 1} \tag{2}$$

(All symbols are defined in Appendix A.)

At top center, all of the mixture with the exception of the minute portion of end gas is assumed to burn at constant volume with no transfer of heat to or from the cylinder walls or to the end gas and with no change in the mean molecular weight of the cylinder contents. This combustion causes an additional adiabatic compression of the end gas resulting in a further increase in temperature and density.

The state of the gas in the cylinder at top center before burning is expressed by the equation for ideal gases,

$$P_c V_c = nRT_c \tag{3}$$

The state of the gas in the cylinder at top center after burning is determined by

$$P_b V_c = nRT_b \tag{4}$$

The combining of equations (3) and (4) results in

$$\frac{P_b}{P_c} = \frac{T_b}{T_c} \tag{5}$$

During constant-volume combustion of the cylinder contents, the small quantity of end gas is adiabatically compressed:

$$\frac{P_k}{P_c} = \left(\frac{T_k}{T_c}\right)^{\frac{\gamma}{\gamma-1}} \tag{6}$$

and

$$\frac{\rho_k}{\rho_c} = \left(\frac{T_k}{T_c}\right)^{\frac{1}{\gamma-1}} \tag{7}$$

The term "effective" has been applied to the knock-limited end-gas temperature and density as calculated by this method because they are based on an idealized air-cycle analysis and differ from the true values. These effective values are of interest principally as a convenient device for correlating knock data.

At a condition of incipient knock, the quantity of mixture that is unburned, comprising the end gas, is assumed to be small. Knock occurs just prior to the complete combustion of the cylinder contents and P_b can be substituted for P_k in equation (6). Thus,

$$\frac{P_b}{P_c} = \left(\frac{T_k}{T_c}\right)^{\frac{\gamma}{\gamma-1}} \tag{8}$$

Then, combining equations (5) and (8) yields

$$T_k = T_c\left(\frac{T_b}{T_c}\right)^{\frac{\gamma-1}{\gamma}} \tag{9}$$

however,

$$T_b = T_c + \Delta T \tag{10}$$

and therefore

$$T_k = T_c\left(1 + \frac{\Delta T}{T_c}\right)^{\frac{\gamma-1}{\gamma}} \tag{11}$$

In references 1 and 2, it is shown that knock-limited performance data for changes in compression ratio and inlet-air temperature can be correlated by means of knock-limited end-gas density and temperature. The assumption is made herein that a relation exists between effective end-gas density and effective end-gas temperature for the incipient-knock condition, which includes the effects of variations of fuel-air ratio, compression ratio, and inlet-air temperature:

$$\rho_k = F_1(T_k) \tag{12}$$

The validity of the assumption is checked by determining the accuracy of correlation obtained by the relation resulting from this assumption.

Equations (7) and (12) may then be combined:

$$\rho_c \left(\frac{T_k}{T_c}\right)^{\frac{1}{\gamma-1}} = F_1(T_k) \tag{13}$$

then

$$\frac{\rho_c}{T_c^{\frac{1}{\gamma-1}}} = \frac{F_1(T_k)}{T_k^{\frac{1}{\gamma-1}}} \tag{14}$$

A function of T_k divided by $T_k^{\frac{1}{\gamma-1}}$, however, becomes merely another function of T_k

$$\frac{\rho_c}{T_c^{\frac{1}{\gamma-1}}} = F_2(T_k) \tag{15}$$

For convenience, the quantity $\rho_c / T_c^{\frac{1}{\gamma-1}}$ will be substituted by the term Z. Replacing T_k in equation (15) by its equivalent in equation (11) gives

$$Z = F_2 \left[T_c\left(1 + \frac{\Delta T}{T_c}\right)\right]^{\frac{\gamma-1}{\gamma}} \tag{16}$$

The term ΔT, the constant-volume temperature rise due to burning of the mixture, is dependent upon many factors, such as fuel-air ratio and the pressure and the temperature of the mixture before burning. The knock-limited data that were to be correlated involved a wide range of compression-air temperatures, densities, and fuel-air ratios with corresponding variation in the temperature rise due to constant-volume combustion. Because fuel-air ratio is the most important factor affecting ΔT, as a first approximation, ΔT was considered to be a function of fuel-air ratio alone. At some reference fuel-air ratio, the temperature rise can be taken as a constant. The reference fuel-air ratio used herein was chosen as 0.08. From thermodynamic charts of reference 4, a

value of 4040° F was chosen as a constant-volume combustion-temperature rise representative of the wide range of engine conditions that were to be correlated. At any fuel-air ratio, the constant-volume temperature rise due to combustion becomes

$$\Delta T = 4040 \; F_3(f) \tag{17}$$

This value for ΔT can then be substituted in equation (16):

$$Z = F_2 \left\{ T_c \left[1 + \frac{4040 \; F_3(f)}{T_c} \right]^{\frac{\gamma-1}{\gamma}} \right\} \tag{18}$$

The method of determining $F_3(f)$ from equation (18) and the engine-knock data is discussed and illustrated in RESULTS AND DISCUSSION.

From equations (1), (2), (7), (11), and (17), the following expressions may be written for the knock-limited effective end-gas temperature and density:

$$T_k = T_0(r)^{\gamma-1} \left[1 + \frac{4040 \; F_3(f)}{T_0(r)^{\gamma-1}} \right]^{\frac{\gamma-1}{\gamma}} \tag{19}$$

$$\rho_k = \frac{W}{V_c r} \left(\frac{T_k}{T_0} \right)^{\frac{1}{\gamma-1}} \tag{20}$$

When the function $F_3(f)$ is known, the end-gas conditions T_k and ρ_k may be computed from equations (19) and (20) by use of the engine data for inlet-air temperature, compression ratio, fuel-air ratio, and air flow obtained at incipient-knock conditions. These values of ρ_k are plotted against T_k for runs in which T_0, r, and f are varied. If a single curve is obtained, regardless of whether T_0, r, or f are varied, the method described will be considered useful in knock-data correlation.

RESULTS AND DISCUSSION

Determination of $F_3(f)$. - Values of Z for variation in fuel-air ratio, compression ratio, and inlet-air temperature are plotted against compression-air temperature in figure 4 for 28-R fuel data obtained on a CFR engine. The values of Z were computed from $\rho_c/T_c^{\frac{1}{\gamma-1}}$ and a constant γ of 1.4 was used. The effect of the vaporization of the injected fuel in the manifold and cylinder on T_c was disregarded. The data covered a range of compression ratios from 5 to 10 at a constant inlet-air temperature of 250° F and a range of inlet-air temperatures from 100° to 350° F at a compression ratio of 8. At each of these conditions the fuel-air ratio was varied between 0.060 and 0.110. A constant spark advance of 30° B.T.C., a coolant temperature of 250° F, and an engine speed of 1800 rpm were maintained in all cases. Curves are faired through all data points having the same fuel-air ratio.

If the quantity Z is arbitrarily held constant, as shown by the horizontal line on figure 4, a single value of compression-air temperature is determined for each fuel-air ratio. For constant Z, the term in braces on the right of equation (18) is constant regardless of fuel-air ratios and the following equation may be written:

$$T_c \left[1 + \frac{4040\ F_3(f)}{T_c} \right]^{\frac{\gamma-1}{\gamma}} = T_{c,0.08} \left(1 + \frac{4040}{T_{c,0.08}} \right)^{\frac{\gamma-1}{\gamma}} \quad (21)$$

The left side of equation (21) pertains to any fuel-air ratio, whereas the right side concerns a fuel-air ratio of 0.08, where the function of fuel-air ratio has been taken as unity. The value of T_c at each fuel-air ratio to be used in solving equation (21) for $F_3(f)$ may be read from figure 4 along the horizontal line of constant Z.

In figure 4, the value of Z for the computation of $F_3(f)$ is chosen to give about the same number of data points on either side of this value. The effect of the choice made for constant Z on the correlation being developed will be subsequently discussed.

The variation of the function of fuel-air ratio with fuel-air ratio was determined in the same manner from knock-limited data for seven other fuels tested in a CFR engine. The following fuels

1225

were used: aviation alkylate, S reference fuel, diisopropyl, triptane, cyclohexane, cyclopentane, and triptene. All these fuels were leaded to 4 ml TEL per gallon. The data for these fuels were obtained over approximately the same range of conditions as for 28-R fuel. Compression-air density and temperature calculations for these data and for 28-R fuel are reported in reference 5.

In figure 5, the functions of fuel-air ratio are plotted against fuel-air ratio for all the fuels, including 28-R fuel. A line has been drawn through the mean of the data. The function of fuel-air ratio may be expected to differ among various fuels; therefore, the use of the function of fuel-air ratio determined for each fuel in a particular engine is advocated when correlating the data for that fuel. When the curve of the function of fuel-air ratio against the fuel-air ratio is unavailable for a fuel, the mean curve, plotted through the data in figure 5, may be used as an approximation. The relative accuracies involved in using the mean curve and the individual curve of the function of fuel-air ratio to correlate the data for a given fuel will be subsequently considered.

Presentation and comparison of correlations. - Knock-limited effective end-gas density and temperature were calculated for all the knock-limited data of the eight fuels. The individual values of the function of fuel-air ratio $F_3(f)$ (fig. 5) for each fuel were employed in making the calculations and the values of T_k and ρ_k were computed from equations (19) and (20). In equation (20), residuals were disregarded in calculating W the weight of cylinder contents per cycle. The correlations are shown in figure 6. The data obtained when the inlet-air temperature was varied are shown by the plain points; whereas the tailed points denote variation of compression ratio. The range of the compression ratio was from 5 to 10, the inlet-air temperature from 100° to 350° F, and the fuel-air ratio from approximately 0.060 to 0.110. One of the checks of the correlation was determined by how well the plain and tailed points fell along a single curve. Because of the great number of points on each plot, only fuel-air ratio was identified for each point. The correlations on the basis of knock-limited effective end-gas density and knock-limited effective end-gas temperature were good for all of the fuels with the exception of the low end-gas temperature region of triptane. The correlation for triptane at high knock-limited effective end-gas temperatures was good but at low knock-limited effective end-gas temperatures considerable scatter occurred. The data at the low knock-limited

effective end-gas temperatures were largely preignition-limited
rather than knock-limited; hence, good correlation could not be
expected.

Unpublished data were available for the performance of 28-R fuel
in an air-cooled full-scale cylinder at compression ratios of 6.7,
7.4, and 8.0, inlet-air temperatures of 150, 200, 250, and 300° F,
and over a range of fuel-air ratios from 0.06 to 0.10. The corre-
lation on the basis of knock-limited effective end-gas density and
knock-limited effective end-gas temperature for the full-scale
cylinder is shown in figure 7. For comparison, the faired curve
from the correlation for 28-R fuel on the CFR engine given in
figure 6 (a) is repeated in figure 7. Exact agreement of the per-
formance of the two cylinders could not be expected because of
differences in cylinder size, cooling, and valve overlap. The
function of fuel-air ratio determined for 28-R fuel in the full-
scale single cylinder was within 6 percent of that for 28-R fuel
in the CFR cylinder at all fuel-air ratios except 0.06, where the
deviation was 20 percent. This correlation suggests the possibility
that the function of fuel-air ratio for a fuel, as determined in one
engine, may apply to the same fuel in other engines for richer-than-
stoichiometric mixtures. A more thorough check is necessary, how-
ever, before such a conclusion can be made.

The faired curves for the eight fuels tested in the CFR engine
are replotted in figure 8; the points are omitted. At mild opera-
ting conditions, as indicated by low knock-limited effective end-
gas temperatures, there is a large difference in the knock-limited
performance of the different fuels. At the severe conditions, the
differences are small but significant. The fuels that are best at
mild conditions tend to have steeper slopes and their advantage
over the other fuels tends to decrease upon approaching more severe
conditions, represented by higher knock-limited effective end-gas·
temperatures.

Method of comparing knock-limited charge flows at various
conditions from correlation curves. - A method of. comparing
knock-limited charge flow W at any desired inlet condition, for
fuels whose curves of knock-limited effective end-gas density
plotted against knock-limited effective end-gas temperature are
known, is presented in figure 9. For clarity, only the knock-
limited curves for 28-R fuel, diisopropyl, and triptane, obtained
from figures 6(a), 6(d), and 6(e), respectively, are replotted in
figure 9.

From equation (20) and the relation

$$V_c r = V_t$$

the following equation may be written:

$$\rho_k = \frac{W}{V_t(T_o)^{\frac{1}{\gamma-1}}} (T_k)^{\frac{1}{\gamma-1}} \tag{22}$$

From equations (1) and (2), $W/V_t(T_o)^{\frac{1}{\gamma-1}}$, appearing as part

of equation (22), is equivalent to $\rho_c/T_c^{\frac{1}{\gamma-1}}$, which has been defined as Z. In the following discussion, however, Z will not be substituted for $W/V_t(T_o)^{\frac{1}{\gamma-1}}$ because the terms comprising this factor are emphasized.

Lines of constant $W/V_t(T_o)^{\frac{1}{\gamma-1}}$, computed from equation (22), are shown superimposed on the curves of knock-limited effective end-gas density plotted against knock-limited effective end-gas temperature in figure 9. Lines of knock-limited effective end-gas temperature T_k plotted against compression-air temperature $T_o(r)^{\gamma-1}$ for constant values of $F_3(f)$ from 0.5 to 1.4, computed from equation (19), are also shown in figure 9.

In order to compare the knock-limited charge flows of the fuels at any condition of inlet-air temperature, compression ratio, and fuel-air ratio, the compression-air temperature $T_o(r)^{\gamma-1}$ is first computed. For the example shown in figure 9, a compression ratio of 8.7 and an inlet-air temperature of 250° F were chosen, which gives a compression-air temperature of 1688° R, as indicated by the dashed horizontal line.

From figure 5, $F_3(f)$ can be read for the fuel-air ratio
desired. Either the mean value of $F_3(f)$ represented by the line
or the individual value for each fuel shown by the data points can
be used. The use of the individual value is, however, more accurate.
For the example presented, the mean value of $F_3(f)$ at a fuel-air
ratio of 0.11 was found to be 0.688 from figure 5. A knock-limited
effective end-gas temperature of 2230° R is found in figure 9 by
proceeding horizontally at 1688° R and interpolating between values
of $F_3(f)$ equal to 0.6 and 0.7. At a knock-limited effective end-

gas temperature of 2230° R, the following values of $W/V_t(T_o)^{\frac{1}{\gamma-1}}$
are found at the intersection with the knock-correlation curves of

the several fuels: 28-R fuel, 3.3×10^{-12}; diisopropyl, 5.2×10^{-12};

triptane, 12.4×10^{-12}. Because compression ratio r, displacement
volume V_t, and inlet-air temperature T_o are held constant, the
knock-limited charge flows W for the several fuels are then in

the same ratio as the values of $W/V_t(T_o)^{\frac{1}{\gamma-1}}$. Likewise, the knock-
limited inlet manifold pressure, which is nearly proportional to
the knock-limited charge flow, is approximately in the same ratio

as the values of $W/V_t(T_o)^{\frac{1}{\gamma-1}}$ for the several fuels.

Determination of indicated mean effective pressure. - If the

indicated specific fuel consumption and the value of $W/V_t(T_o)^{\frac{1}{\gamma-1}}$
are known for a fuel at some desired condition, the indicated mean
effective pressure can be calculated. The equation, developed in
appendix B, is

$$\text{imep} = 2.376 \times 10^7 \left[\frac{W}{V_t(T_o)^{\frac{1}{\gamma-1}}} \right] (T_o)^{\frac{1}{\gamma-1}} \quad \frac{r}{r-1} \quad \frac{f}{1+f} \quad \frac{1}{\text{isfc}} \quad (23)$$

In order to simplify the computation of indicated mean effective

pressure from values of $W/V_t(T_o)^{\frac{1}{\gamma-1}}$ read from figure 9, a chart
based on equation (23) is presented in figure 10. Use of this chart
is illustrated by computing the indicated mean effective pressure

of diisopropyl at a compression ratio of 8.7, an inlet-air temperature of 250° F, and a fuel-air ratio of 0.11, which are the conditions used for the example in figure 9.

The value of $W/V_t(T_o)^{\frac{1}{\gamma-1}}$ at this condition for diisopropyl was found to be 5.2 × 10⁻¹². From the left of the chart (fig. 10) at this value of $W/V_t(T_o)^{\frac{1}{\gamma-1}}$, follow the compression ratio lines until a compression ratio of 8.7 is reached. From this point, proceed horizontally across the chart to the inlet-air-temperature line of 710° R (corresponding to 250° F) and then vertically upward until the indicated-specific-fuel-consumption line for this condition is reached. The indicated specific fuel consumption of diisopropyl in a CFR engine at the stated conditions was found to be 0.625 pound per horsepower-hour from previous runs (reference 5). By proceeding horizontally from the indicated-specific-fuel-consumption line to the fuel-air-ratio line of 0.11, the indicated mean effective pressure is found to be 300 pounds per square inch.

Accuracy of correlation. - The error of the correlation method was obtained by comparing the value of the knock-limited charge flow computed from the correlation curve with the value observed in the engine runs for all the conditions and fuels investigated. The end-gas density-temperature correlation curves for all the fuels (fig. 6) were superimposed on figure 9. Individual values of $F_3(f)$ for each fuel were used and the knock-limited charge flows were determined from figure 9 for each fuel at fuel-air ratios of 0.06, 0.07, 0.08, 0.09, 0.10, and 0.11 at each of the six compression ratios and five inlet-air temperatures. These values, in addition to the measured values of knock-limited charge flow derived from the air-flow curves for the actual engine data, are presented in table I. The percentage error

$$100 \cdot \frac{\text{calculated } W - \text{measured } W}{\text{measured } W}$$

is tabulated without regard to sign and is averaged for each fuel. Two averages are given for each fuel, representing data taken at a variable inlet-air temperature or at a variable compression ratio. In the case of triptane, no error is computed for data that fell within the designated preignition zone of figure 6(e). The inclusion of these data would penalize the correlation for the tendency of the engine to run into preignition at high power levels.

The smallest mean error in calculated charge flow encountered was 2.7 percent for S reference fuel under conditions of variable inlet-air temperature. The greatest mean error was 8.6 percent for triptane under similar conditions of variable inlet-air temperature. When the errors in calculated charge flow were averaged for all the fuels at all the operating conditions, the mean was found to be 5.0 percent. The mean error in calculated charge flow at conditions of variable inlet-air temperature is less than the mean error at variable compression ratio for all the fuels except triptane.

Effect of using mean $F_3(f)$ in place of individual $F_3(f)$ on correlation accuracy. - A mean $F_3(f)$ determined in a given engine for a number of fuels might be used, as previously discussed, in establishing the end-gas temperature-density correlation for data on a new fuel when the range of that data is insufficient to compute the individual $F_3(f)$ for the fuel. Use of the mean $F_3(f)$ in determining the correlation curve for each fuel and in computing knock-limited charge flow from the correlation curve may be an additional source of error. Consequently, knock-limited charge flows were computed from the correlation curves of figure 6 by use of figure 9 and the mean curve of the function of fuel-air ratio (fig. 5). The conditions for which the knock-limited charge flows were determined were the same as those listed in table I. The mean error in calculated charge flow using the mean $F_3(f)$ was then found for each fuel at variable inlet-air temperature and at variable compression ratio. These values are compared in table II with the mean error in calculated charge flow using the individual $F_3(f)$ values, taken from table I. The individual curve of $F_3(f)$ resulted in the least error in all cases except two, diisopropyl at variable compression ratio and cyclopentane at variable inlet-air temperature. In some cases, the additional mean error in calculated charge flow caused by using mean $F_3(f)$ instead of individual $F_3(f)$ is small. Triptane, however, shows a great increase in mean error resulting from its extreme sensitivity to change of operating conditions. Because of the steep slope of the correlation curve for triptane, deviation of the individual value of $F_3(f)$ from the mean value of $F_3(f)$ at the lower fuel-air ratios is responsible for a greater variation in calculated charge flow than that obtained when the same amount of deviation in $F_3(f)$ occurs with a less-sensitive fuel of lower slope. Care must be taken in applying this method of correlation to a very sensitive fuel not only in the selection of $F_3(f)$ but also in the measurement of inlet-air temperature, compression ratio, and other variables of operation.

A mean value of $F_3(f)$ for a number of fuels in a given engine may be used in computing data when an individual value of $F_3(f)$ for a new fuel is unavailable. If known, however, the individual curve of the function of fuel-air ratio for a fuel on a given engine should be used in order to obtain the best estimates of knock-limited charge flow.

Effect of choice of Z on correlation. - The possibility has been mentioned that the value of Z at which the function of fuel-air ratio was calculated on the charts where Z is plotted against T_c (fig. 11) might influence the correlations. Consequently, calculations of the function of fuel-air ratio were made for diisopropyl and triptene at values of Z other than those used in the correlations presented in figures 6(d) and 6(h). In the case of diisopropyl, the functions of fuel-air ratio used for the correlation in figure 6(d) were determined at a value of $Z = 6 \times 10^{-12}$. Additional determinations were then made at $Z = 3.5 \times 10^{-12}$ and $Z = 11 \times 10^{-12}$, as indicated on the plot of Z in figure 11(a). With diisopropyl, the functions of fuel-air ratio determined at the low and high values of Z were expected to differ considerably for the higher fuel-air ratios because of the great difference in the values of $T_{c,0.11}/T_{c,0.08}$ for the high and low values of Z.

For triptene, the functions of fuel-air ratio used in the correlation on figure 6(h) were determined at $Z = 4 \times 10^{-12}$ and the additional calculations were made at $Z = 2 \times 10^{-12}$ and $Z = 6.5 \times 10^{-12}$ (fig. 11(b)). In the case of triptene, the differences in $T_{c,0.11}/T_{c,0.08}$ for the high and low values of Z were much less than for diisopropyl. Consequently, the choice of Z in calculating the function of fuel-air ratio for triptene was expected to have less effect on the function of fuel-air ratio than it did in the case of diisopropyl.

Results of the computation of the function of fuel-air ratio at three values of Z for diisopropyl and triptene are presented in table III. At a fuel-air ratio of 0.11, the functions of fuel-air ratio computed at different values of Z vary much less for triptene than for diisopropyl. The same conclusion can be reached concerning all the fuel-air ratios above 0.08. At a fuel-air ratio of 0.06, however, there is less variation in the function of fuel-air ratio with diisopropyl than with triptene.

In figures 12(a) and 12(b), curves of knock-limited effective end-gas density plotted against knock-limited effective end-gas temperature for diisopropyl that are computed from the function of

fuel-air ratio for $Z = 3.5 \times 10^{-12}$ and $Z = 11 \times 10^{-12}$, respectively, are presented. Figures 13(a) and 13(b) present the curves of knock-limited effective end-gas density plotted against knock-limited effective end-gas temperature for triptene, computed from the function of fuel-air ratio determined for $Z = 2.0 \times 10^{-12}$ and $Z = 6.5 \times 10^{-12}$, respectively.

The curve for diisopropyl, based on the function of fuel-air ratio at $Z = 3.5 \times 10^{-12}$, (fig. 12(a)), involves some scatter at the low knock-limited effective end-gas temperatures. When the function of fuel-air ratio is determined at a $Z = 11 \times 10^{-12}$, however, the scatter at the low knock-limited effective end-gas temperatures is reduced but there is an increase in the scatter at the higher knock-limited effective end-gas temperatures. Some shifting also occurs in the position of the curve. These effects are caused by the change in the function of fuel-air ratio with change in Z that takes place at the rich fuel-air ratios with diisopropyl. Comparison of figures 12(a) and 12(b) with figure 6(d) (which was obtained using an $F_3(f)$ curve based on $Z = 6 \times 10^{-12}$) indicates that the use of the intermediate value of Z in determining $F_3(f)$ appears to give the best correlation.

The curves of knock-limited effective end-gas density plotted against knock-limited effective end-gas temperature for triptene (fig. 13(a) and 13(b)) calculated from the function of fuel-air ratio at $Z = 2.0 \times 10^{-12}$ and $Z = 6.5 \times 10^{-12}$, are almost identical because of the small effect that change in Z has on the function of fuel-air ratio for triptene.

The choice of Z can have an appreciable effect on both the position and the shape of the curve of knock-limited effective end-gas density plotted against knock-limited effective end-gas temperature. Determination of the value of Z that gives the best correlation for each fuel would, however, involve too lengthy an analysis to be practicable. Hence, the procedure followed in figure 4 of drawing the line of constant Z for the determination of $F_3(f)$ so that an approximately equal number of points fall on each side is recommended. This method is somewhat comparable to choosing Z in the middle range of power levels encountered in procuring the data.

1225

SUMMARY OF RESULTS

A method of correlating the knock-limited charge flow of an engine with inlet-air temperature, compression ratio, and fuel-air ratio was developed and applied to knock data obtained in a supercharged CFR engine with the following fuels: 28-R fuel, aviation alkylate, S reference fuel, diisopropyl, triptane, cyclohexane, cyclopentane, and triptene. A relation between knock-limited effective end-gas density and end-gas temperature calculated from inlet conditions was used to correlate these variables. The effect of variation in fuel-air ratio on knock-limited effective end-gas density and temperature was computed by using a function of fuel-air ratio derived from engine data. Charts are included for determining knock-limited charge flow and indicated mean effective pressure from correlation curves of the variation of knock-limited effective end-gas density with knock-limited effective end-gas temperature.

When these curves of knock-limited effective end-gas density with effective end-gas temperature were used to compute knock-limited charge flow for the eight fuels over a wide range of conditions, good agreement was obtained with experimental values of knock-limited charge flow.

The smallest mean error in knock-limited charge flow, by using the function of fuel-air ratio individually determined for each fuel, was 2.7 percent for S reference fuel under conditions of variable inlet-air temperature. The greatest mean error using the individual function of fuel-air ratio was 8.6 percent for triptane when inlet-air temperature was varied. The mean error in calculated charge flow for all the fuels at all the conditions was 5.0 percent. When the mean value of the function of fuel-air ratio, determined by averaging the individual function of fuel-air ratio for the eight fuels, was used to compute the knock-limited charge flow, the mean error in knock-limited charge flow was higher in nearly all cases. (This result signifies that the individual function of fuel-air ratio should be used when possible.) Evidence was also presented that the accuracy of the correlation can be affected by the manner in which the engine data are used to compute the function of fuel-air ratio.

Lewis Flight Propulsion Laboratory,
     National Advisory Committee for Aeronautics,
          Cleveland, Ohio, March 15, 1949.

APPENDIX A

SYMBOLS

The following symbols are used in this report:

f fuel-air ratio

F_1, F_2, F_3 functions

n moles of gas present in cylinder

P_b pressure of burned mixture at top center, lb/sq in.

P_c compression pressure, lb/sq in.

P_k effective end-gas pressure at instant before knock, lb/sq in.

R universal gas constant, 1545 ft-lb/(mol)($^\circ$F)

r compression ratio

T_b temperature of burned mixture at top center, $^\circ$R

T_c compression-air temperature, $^\circ$R

T_k effective end-gas temperature at instant before knock, $^\circ$R

T_o inlet-air temperature, $^\circ$R

ΔT temperature rise of cylinder contents due to constant-volume burning, $^\circ$F

V_c clearance volume, cu in.

V_d displacement volume, cu in.

V_t total cylinder volume with piston at bottom center, cu in.

W knock-limited charge flow, or weight of fuel and air inducted per cycle, lb/cycle

W_a air flow, lb/cycle

W_f fuel flow, lb/cycle

Z factor replacing $\rho_c / T_c^{\frac{1}{\gamma-1}}$

γ ratio of specific heat at constant pressure to specific heat at constant volume

ρ_c compression charge density, lb/cu in.

ρ_k effective end-gas density at instant before knock, lb/cu in.

APPENDIX B

CALCULATIONS

Derivation of the following equation for indicated mean effective pressure is given:

$$\text{imep} = 2.376 \times 10^7 \left(\frac{W}{V_t (T_0)^{\frac{1}{\gamma-1}}} \right) (T_0)^{\frac{1}{\gamma-1}} \frac{r}{r-1} \frac{f}{1+f} \frac{1}{\text{isfc}} \qquad (23)$$

The familiar expression for horsepower is

$$\text{hp} = \frac{p\ l\ a\ n}{550} \qquad (A1)$$

where

p   cylinder pressure, lb/sq ft

l   piston stroke, ft

a   piston area, sq ft

n   intake or firing strokes per sec

or for indicated horsepower

$$\text{ihp} = \frac{\text{imep } V_d\ n}{12 \times 550} \qquad (A2)$$

The definition of indicated specific fuel consumption

$$\text{isfc} = \frac{3600\ n\ W_f}{\text{ihp}} \qquad (A3)$$

Combining equations (A2) and (A3) gives

$$\text{imep} = \frac{12 \times 3600 \times 550\ W_f}{V_d\ \text{isfc}} \qquad (A4)$$

Multiplying by $(W_f + W_a)/(W_f + W_a)$ yields

$$\text{imep} = \frac{12 \times 3600 \times 550 \ (W_f + W_a)}{V_d \ \text{isfc}} \ \frac{W_f}{W_f + W_a} \qquad (A5)$$

However, $V_d = V_t \ (r\text{-}1)/r$ and $W_f + W_a = W$. Therefore,

$$\text{imep} = \frac{2.376 \times 10^7}{\text{isfc}} \ \frac{W}{V_t} \ \frac{r}{r\text{-}1} \ \frac{f}{1+f} \qquad (A6)$$

where

$$f = W_a/W_f$$

Multiplying by $T_o^{\frac{1}{\gamma-1}}/T_o^{\frac{1}{\gamma-1}}$ gives

$$\text{imep} = 2.376 \times 10^7 \ \frac{W}{V_t(T_o)^{\frac{1}{\gamma-1}}} \ (T_o)^{\frac{1}{\gamma-1}} \ \frac{r}{r\text{-}1} \ \frac{f}{1+f} \ \frac{1}{\text{isfc}} \qquad (23)$$

REFERENCES

1. Rothrock, A. M., and Biermann, Arnold E.: The Knocking Characteristics of Fuels in Relation to Maximum Permissible Performance of Aircraft Engines. NACA Rep. 655, 1939.

2. Taylor, E. S., Leary, W. A., and Diver, J. R.: Effect of Fuel-Air Ratio, Inlet Temperature, and Exhaust Pressure on Detonation. NACA Rep. 699, 1940.

3. Evvard, John C., and Branstetter, J. Robert: A Correlation of the Effects of Compression Ratio and Inlet-Air Temperature on the Knock Limits of Aviation Fuels in a CFR Engine - I. NACA ACR E5D20, 1945.

4. Hershey, R. L., Eberhardt, J. E., and Hottel, H. C.: Thermodynamic Properties of the Working Fluid in Internal-Combustion Engines. S.A.E. Jour. (Trans.), vol. 39, no. 4, Oct. 1936, pp. 409-424.

5. Alquist, Henry E., O'Dell, Leon, and Evvard, John C.: A Correlation of the Effects of Compression Ratio and Inlet-Air Temperature on the Knock Limits of Aviation Fuels in a CFR Engine - II. NACA ARR E6E13, 1946.

TABLE I – COMPARISON OF CALCULATED AND MEASURED KNOCK-LIMITED CHARGE FLOW IN SUPERCHARGED CFR ENGINE

(a) 28-R fuel.

Fuel-air ratio f	Variable inlet-air temperature						Variable compression ratio				
	Inlet-air temperature T_0 (°F)	Compression ratio r	Knock-limited charge flow W (lb/cycle)		Charge flow error (percent) (a)	Inlet-air temperature T_0 (°F)	Compression ratio r	Knock-limited charge flow W (lb/cycle)		Charge flow error (percent) (a)
			Calculated	Measured				Calculated	Measured	
0.06	100	8.0	1.776×10^{-3}	1.833×10^{-3}	3.1	250	5.0	3.052×10^{-3}	3.247×10^{-3}	6.0
.07			1.713	1.747	2.0			2.876	3.140	8.4
.08			1.897	1.940	2.2			3.240	3.400	4.7
.09			2.119	2.127	.4			3.667	3.773	2.8
.10			2.325	2.260	2.9			3.962	4.013	1.3
.11			2.474	2.313	7.0			4.263	4.047	5.3
0.06	150	8.0	1.725×10^{-3}	1.673×10^{-3}	3.1	250	6.0	2.304×10^{-3}	2.273×10^{-3}	1.4
.07			1.603	1.620	1.0			2.165	2.227	2.8
.08			1.807	1.853	2.5			2.443	2.600	6.0
.09			2.063	2.067	.2			2.816	2.927	3.8
.10			2.275	2.227	2.2			3.112	3.100	.4
.11			2.424	2.313	4.8			3.341	3.187	4.8
0.06	200	8.0	1.588×10^{-3}	1.580×10^{-3}	0.5	250	7.3	1.658×10^{-3}	1.540×10^{-3}	7.7
.07			1.512	1.453	4.1			1.535	1.407	9.1
.08			1.674	1.713	2.3			1.774	1.713	3.6
.09			1.952	1.960	.4			2.041	2.033	.4
.10			2.172	2.147	1.2			2.274	2.287	.6
.11			2.311	2.260	2.3			2.501	2.447	2.2
0.06	250	8.0	1.413×10^{-3}	1.407×10^{-3}	0.4	250	8.7	1.180×10^{-3}	1.087×10^{-3}	8.6
.07			1.309	1.300	.7			1.101	1.033	6.6
.08			1.499	1.527	1.8			1.305	1.260	3.6
.09			1.769	1.767	.1			1.510	1.487	1.6
.10			1.998	1.973	1.3			1.708	1.700	.5
.11			2.136	2.153	.8			1.878	1.893	.8
0.06	300	8.0	1.205×10^{-3}	1.160×10^{-3}	3.9	250	10.0	0.871×10^{-3}	0.800×10^{-3}	8.9
.07			1.089	1.160	6.1			.787	.727	8.2
.08			1.307	1.413	7.5			.960	.953	.7
.09			1.559	1.660	6.1			1.139	1.207	5.6
.10			1.770	1.873	5.5			1.312	1.440	8.9
.11			1.940	2.040	4.9			1.445	1.633	11.5
0.06	350	8.0	0.998×10^{-3}	1.007×10^{-3}	0.9					
.07			.910	.973	6.5					
.08			1.078	1.160	7.1					
.09			1.349	1.407	4.1					
.10			1.557	1.707	8.8					
.11			1.700	2.033	16.4					
Mean error					3.5					4.6

a Error listed without regard for sign.

TABLE I – COMPARISON OF CALCULATED AND MEASURED KNOCK-LIMITED CHARGE FLOW IN SUPERCHARGED CFR ENGINE – Continued

(b) Aviation alkylate.

Fuel-air ratio f	Variable inlet-air temperature					Variable compression ratio				
	Inlet-air temperature T_0 (°F)	Compression ratio r	Knock-limited charge flow W (lb/cycle)		Charge-flow error (percent) (a)	Inlet-air temperature T_0 (°F)	Compression ratio r	Knock-limited charge flow W (lb/cycle)		Charge-flow error (percent) (a)
			Calculated	Measured				Calculated	Measured	
0.06	100	8.0	2.211×10^{-3}	2.287×10^{-3}	3.3	250	5.0	3.755×10^{-3}	3.693×10^{-3}	1.7
.07			1.998	2.080	3.9			3.384	3.320	1.9
.08			2.033	2.133	4.7			3.447	3.453	.2
.09			2.284	2.240	2.0			3.818	3.787	.8
.10			2.458	2.373	3.6			4.113	3.980	3.3
.11			2.531	2.473	2.4			4.257	4.080	4.3
0.06	150	8.0	2.094×10^{-3}	2.173×10^{-3}	3.6	250	6.0	2.877×10^{-3}	2.713×10^{-3}	6.0
.07			1.878	1.947	3.5			2.581	2.453	5.2
.08			1.925	2.020	4.7			2.642	2.540	4.0
.09			2.149	2.167	.8			2.925	2.753	6.2
.10			2.298	2.300	.1			3.136	2.960	6.0
.11			2.357	2.400	1.8			3.251	3.120	4.2
0.06	200	8.0	1.985×10^{-3}	2.007×10^{-3}	1.1	250	7.3	2.140×10^{-3}	2.133×10^{-3}	0.3
.07			1.794	1.807	.7			1.966	1.867	5.3
.08			1.827	1.887	3.2			1.989	1.953	1.8
.09			2.028	2.020	.4			2.210	2.087	5.9
.10			2.143	2.153	.5			2.321	2.253	3.0
.11			2.248	2.260	.5			2.408	2.427	.8
0.06	250	8.0	1.912×10^{-3}	1.867×10^{-3}	2.4	250	8.7	1.697×10^{-3}	1.613×10^{-3}	5.2
.07			1.746	1.660	5.2			1.504	1.395	8.0
.08			1.774	1.813	2.2			1.566	1.527	2.6
.09			1.941	1.967	1.3			1.748	1.700	2.8
.10			2.061	2.100	1.9			1.844	1.847	.2
.11			2.107	2.173	3.0			1.872	1.967	4.8
0.06	300	8.0	1.783×10^{-3}	1.667×10^{-3}	7.0	250	10.0	1.334×10^{-3}	1.153×10^{-3}	15.7
.07			1.552	1.407	10.3			1.155	1.073	7.6
.08			1.615	1.567	2.9			1.189	1.193	.3
.09			1.858	1.780	3.3			1.367	1.373	.4
.10			2.001	1.953	2.5			1.507	1.540	2.1
.11			2.042	2.073	1.5			1.552	1.680	7.6
0.06	350	8.0	1.541×10^{-3}	1.460×10^{-3}	5.6					
.07			1.261	1.220	3.4					
.08			1.341	1.387	3.3					
.09			1.597	1.600	.2					
.10			1.772	1.787	.8					
.11			1.828	1.960	6.7					
Mean error					2.9					3.9

aError listed without regard for sign.

TABLE I – COMPARISON OF CALCULATED AND MEASURED KNOCK-LIMITED CHARGE FLOW IN SUPERCHARGED CFR ENGINE – Continued

(c) S reference fuel.

Variable inlet-air temperature

Fuel-air ratio f	Inlet-air temperature T (°F)	Compression ratio r	Knock-limited charge flow W (lb/cycle)		Charge-flow error (percent) (a)
			Calculated	Measured	
0.06	100	8.0	2.718×10^{-3}	2.907×10^{-3}	6.5
.07			2.344	2.467	5.0
.08			2.481	2.520	1.6
.09			2.664	2.640	.9
.10			2.918	2.787	4.7
.11			3.124	2.907	7.5
0.06	150	8.0	2.589×10^{-3}	2.833×10^{-3}	8.6
.07			2.208	2.300	4.0
.08			2.338	2.340	.1
.09			2.511	2.493	.7
.10			2.790	2.653	5.2
.11			2.978	2.827	5.3
0.06	200	8.0	2.402×10^{-3}	2.353×10^{-3}	2.1
.07			2.057	2.053	.2
.08			2.153	2.173	.9
.09			2.363	2.340	1.0
.10			2.622	2.520	4.0
.11			2.803	2.687	4.3
0.06	250	8.0	2.182×10^{-3}	2.280×10^{-3}	4.3
.07			1.855	1.860	.3
.08			1.947	1.967	1.0
.09			2.159	2.160	0
.10			2.406	2.360	2.0
.11			2.595	2.553	1.6
0.06	300	8.0	1.967×10^{-3}	1.860×10^{-3}	5.8
.07			1.627	1.567	3.8
.08			1.756	1.747	.5
.09			1.947	1.960	.7
.10			2.165	2.173	.4
.11			2.342	2.353	.5
0.06	350	8.0	1.732×10^{-3}	1.680×10^{-3}	3.1
.07			1.397	1.347	3.7
.08			1.493	1.500	.5
.09			1.708	1.753	2.6
.10			1.916	1.953	1.9
.11			2.115	2.127	.6
Mean error					2.7

Variable compression ratio

Fuel-air ratio f	Inlet-air temperature T (°F)	Compression ratio r	Knock-limited charge flow W (lb/cycle)		Charge-flow error (percent) (a)
			Calculated	Measured	
0.06	250	5.0	4.646×10^{-3}	4.987×10^{-3}	6.8
.07			3.949	4.267	7.4
.08			4.157	4.427	6.1
.09			4.508	4.633	2.7
.10			4.960	4.867	1.9
.11			5.268	5.121	2.9
0.06	250	6.0	3.510×10^{-3}	3.620×10^{-3}	3.0
.07			3.016	3.020	.1
.08			3.184	3.127	1.8
.09			3.450	3.420	.9
.10			3.751	3.680	1.9
.11			4.071	3.887	4.7
0.06	250	7.3	2.559×10^{-3}	2.500×10^{-3}	2.4
.07			2.181	2.127	2.5
.08			2.297	2.273	1.1
.09			2.478	2.520	1.7
.10			2.728	2.733	.2
.11			3.018	2.907	3.8
0.06	250	8.7	1.901×10^{-3}	1.960×10^{-3}	3.0
.07			1.589	1.627	2.3
.08			1.674	1.727	3.1
.09			1.861	1.927	3.4
.10			2.049	2.140	4.2
.11			2.213	2.333	5.1
0.06	250	10.0	1.445×10^{-3}	1.453×10^{-3}	0.6
.07			1.211	1.193	1.5
.08			1.295	1.327	2.4
.09			1.434	1.580	9.2
.10			1.607	1.807	11.1
.11			1.758	2.007	12.4
					3.7

aError listed without regard for sign.

1225

TABLE I – COMPARISON OF CALCULATED AND MEASURED KNOCK-LIMITED CHARGE FLOW IN SUPERCHARGED CFR ENGINE – Continued

(d) Diisopropyl.

Variable inlet-air temperature

Fuel-air ratio f	Inlet-air temperature T_0 (°F)	Compression ratio r	Knock-limited charge flow W (lb/cycle) Calculated	Knock-limited charge flow W (lb/cycle) Measured	Charge-flow error (percent) (a)
0.06	100	8.0	3.553×10^{-3}	3.887×10^{-3}	8.6
.07			3.486	3.767	7.5
.08			3.870	4.033	4.0
.09			4.276	4.247	.7
.10			(b)	4.320	---
.11			(b)	4.233	---
0.06	150	8.0	3.033×10^{-3}	3.160×10^{-3}	4.0
.07			2.947	2.927	.7
.08			3.371	3.420	1.4
.09			3.831	3.740	2.4
.10			4.243	3.960	7.2
.11			4.707	4.120	14.2
0.06	200	8.0	2.473×10^{-3}	2.440×10^{-3}	1.4
.07			2.392	2.327	2.8
.08			2.727	2.753	.9
.09			3.224	3.180	1.4
.10			3.636	3.587	1.4
.11			4.124	3.860	6.8
0.06	250	8.0	1.883×10^{-3}	1.820×10^{-3}	3.5
.07			1.809	1.800	.5
.08			2.142	2.153	.5
.09			2.526	2.520	.2
.10			2.934	2.913	.7
.11			3.353	3.293	1.8
0.06	300	8.0	1.464×10^{-3}	1.500×10^{-3}	2.4
.07			1.423	1.380	3.1
.08			1.675	1.653	1.3
.09			1.967	1.953	.7
.10			2.301	2.287	.6
.11			2.641	2.647	.2
0.06	350	8.0	1.150×10^{-3}	1.153×10^{-3}	0.3
.07			1.094	1.180	7.3
.08			1.301	1.413	7.9
.09			1.541	1.687	8.6
.10			1.820	2.000	9.0
.11			2.076	2.347	11.6

Mean error: 3.7

Variable compression ratio

Fuel-air ratio f	Inlet-air temperature T_0 (°F)	Compression ratio r	Knock-limited charge flow W (lb/cycle) Calculated	Knock-limited charge flow W (lb/cycle) Measured	Charge-flow error (percent) (a)
0.06	250	5.0	5.701×10^{-3}	(c)	---
.07			5.588	5.700×10^{-3}	2.0
.08			6.279	6.187	1.5
.09			7.120	6.507	9.4
.10			7.842	(c)	---
.11			8.559	(c)	---
0.06	250	6.0	3.872×10^{-3}	4.667×10^{-3}	17.0
.07			3.739	3.840	2.6
.08			4.324	4.247	1.8
.09			4.921	5.087	3.3
.10			5.555	5.573	.3
.11			6.260	(c)	---
0.06	250	7.3	2.373×10^{-3}	2.427×10^{-3}	2.2
.07			2.297	2.333	1.5
.08			2.670	2.707	1.4
.09			3.187	3.133	1.7
.10			3.687	3.593	2.6
.11			4.182	4.087	2.3
0.06	250	8.7	1.532×10^{-3}	1.447×10^{-3}	5.9
.07			1.464	1.427	2.6
.08			1.697	1.720	1.3
.09			2.043	2.080	1.8
.10			2.355	2.480	5.0
.11			2.730	2.900	5.9
0.06	250	10.0	1.049×10^{-3}	0.993×10^{-3}	5.6
.07			1.005	.933	7.7
.08			1.194	1.140	4.7
.09			1.395	1.453	2.6
.10			1.646	1.733	5.0
.11			1.898	2.040	7.0

Mean error: 4.0

aError listed without regard for sign.
bCondition not covered by correlation curve.
cNo engine data available.

NACA

TABLE I – COMPARISON OF CALCULATED AND MEASURED KNOCK-LIMITED CHARGE FLOW IN SUPERCHARGED CFR ENGINE – Continued

(c) Triptane.

	Variable inlet-air temperature					Variable compression ratio				
Fuel-air ratio f	Inlet-air temperature T_0 (°F)	Compression ratio r	Knock-limited charge flow W (lb/cycle) Calculated	Measured	Charge-flow error (percent) (a)	Inlet-air temperature T_0 (°F)	Compression ratio r	Knock-limited charge flow W (lb/cycle) Calculated	Measured	Charge-flow error (percent) (a)
0.06	100	8.0	(b)	(c)	------	250	5.0	(b)	7.707×10^{-3}	------
.07			(b)	(c)	------			(b)	9.433	------
.08			(b)	(c)	------			(b)	10.400	------
.09			(b)	(c)	------			(b)	10.600	------
.10			(b)	(c)	------			(b)	10.500	------
.11			(b)	(c)	------			(b)	10.400	------
0.06	150	8.0	(b)	(c)	------	250	6.0	(b)	6.240×10^{-3}	------
.07			(b)	(c)	------			(b)	7.933	------
.08			(b)	(c)	------			(b)	8.493	------
.09			(b)	(c)	------			(b)	8.527	------
.10			(b)	(c)	------			(b)	(c)	------
.11			(b)	(c)	------			(b)	(c)	------
0.06	200	8.0	4.114×10^{-3}	3.960×10^{-3}	3.9	250	7.3	3.652×10^{-3}	3.553×10^{-3}	2.8
.07			(b)	4.633	------			4.624	4.340	6.5
.08			(b)	5.947	------			(b)	5.940	------
.09			(b)	6.360	------			(b)	6.873	------
.10			(b)	6.433	------			(b)	7.093	------
.11			(b)	6.453	------			(b)	7.140	------
0.06	250	8.0	2.515×10^{-3}	2.620×10^{-3}	4.0	250	8.7	1.754×10^{-3}	2.027×10^{-3}	13.5
.07			3.284	3.033	8.3			2.242	2.213	1.3
.08			4.858	4.520	7.5			3.598	3.440	4.6
.09			(b)	5.607	------			4.869	4.767	2.1
.10			(b)	6.253	------			(b)	5.680	------
.11			(b)	6.453	------			(b)	6.093	------
0.06	300	8.0	1.457×10^{-3}	1.667×10^{-3}	12.6	250	10.0	0.988×10^{-3}	1.127×10^{-3}	12.3
.07			1.892	1.893	0			1.233	1.193	3.4
.08			3.036	3.133	3.1			1.976	1.620	22.0
.09			4.254	4.700	9.5			2.841	2.633	7.9
.10			5.800	6.067	4.4			3.951	3.933	.5
.11			6.909	6.380	8.3			4.738	4.867	2.6
0.06	350	8.0	1.030×10^{-3}	1.133×10^{-3}	9.1					
.07			1.221	1.133	7.8					
.08			1.804	1.553	16.2					
.09			2.555	2.420	5.6					
.10			3.672	5.200	29.4					
.11			4.742	(c)	------					
Mean error					8.6					6.6

a Error listed without regard for sign.
b Point within preignition zone. (See fig. 10.)
c No engine data available.

1225

TABLE I – COMPARISON OF CALCULATED AND MEASURED KNOCK-LIMITED CHARGE FLOW IN SUPERCHARGED CFR ENGINE – Continued

(f) Cyclopentane.

Fuel-air ratio f	Variable inlet-air temperature					Variable compression ratio				
	Inlet-air temperature T_0 (°F)	Compression ratio r	Knock-limited charge flow W (lb/cycle) Calculated	Measured	Charge-flow error (percent) (a)	Inlet-air temperature T_0 (°F)	Compression ratio r	Knock-limited charge flow W (lb/cycle) Calculated	Measured	Charge-flow error (percent) (a)
0.06	100	8.0	2.817×10^{-3}	2.973×10^{-3}	5.2	250	5.0	4.081×10^{-3}	4.340×10^{-3}	5.5
.07			3.070	3.267	6.0			4.395	4.835	9.1
.08			3.759	4.227	11.1			5.212	7.027	25.8
.09			4.821	5.280	8.7			6.593	9.240	28.6
.10			5.773	(c)	----			8.100	(c)	----
.11			(b)	(c)	----			11.300	(c)	----
0.06	150	8.0	2.082×10^{-3}	1.913×10^{-3}	8.8	250	6.0	2.533×10^{-3}	2.613×10^{-3}	3.1
.07			2.220	1.880	18.1			2.714	2.567	5.7
.08			2.632	2.413	9.1			3.196	3.200	.1
.09			3.253	3.053	6.6			3.932	3.947	.4
.10			3.870	3.760	2.9			4.813	4.967	3.1
.11			5.422	4.533	19.6			6.441	6.240	3.2
0.06	200	8.0	1.574×10^{-3}	1.620×10^{-3}	2.8	250	7.3	1.506×10^{-3}	1.427×10^{-3}	5.5
.07			1.670	1.500	11.3			1.617	1.387	16.6
.08			1.971	1.807	9.1			1.896	1.780	6.5
.09			2.449	2.307	6.2			2.338	2.273	2.9
.10			2.846	2.967	4.1			2.716	2.867	5.3
.11			3.789	3.520	7.6			3.594	3.520	2.1
0.06	250	8.0	1.189×10^{-3}	1.267×10^{-3}	6.2	250	8.7	0.976×10^{-3}	0.900×10^{-3}	8.5
.07			1.246	1.187	5.0			1.004	.913	10.0
.08			1.504	1.453	3.5			1.203	1.133	6.2
.09			1.832	1.807	1.4			1.464	1.420	3.1
.10			2.170	2.213	1.9			1.702	1.800	5.4
.11			2.814	2.667	5.5			2.270	2.267	.1
0.06	300	8.0	0.939×10^{-3}	0.967×10^{-3}	2.8	250	10.0	0.686×10^{-3}	0.720×10^{-3}	4.6
.07			.987	.873	13.1			.742	.760	2.3
.08			1.178	1.120	5.2			.837	.907	7.7
.09			1.395	1.400	.4			.999	1.120	10.8
.10			1.654	1.713	3.4			1.144	1.380	17.1
.11			2.165	2.027	6.8			1.507	1.680	10.3
0.06	350	8.0	0.838×10^{-3}	0.835×10^{-3}	0.6					
.07			.870	.820	6.1					
.08			.958	.980	2.2					
.09			1.102	1.247	11.6					
.10			1.301	1.587	18.0					
.11			1.660	1.973	15.9					
Mean error					7.3					7.5

a Error listed without regard for sign.
b Condition not covered by correlation curve.
c No engine data available.

1225

TABLE I – COMPARISON OF CALCULATED AND MEASURED KNOCK-LIMITED CHARGE FLOW IN SUPERCHARGED CFR ENGINE – Continued

(g) Cyclohexane.

Variable inlet-air temperature

Fuel-air ratio f	Inlet-air temperature T (°F)	Compression ratio r	Knock-limited charge flow W (lb/cycle) Calculated	Knock-limited charge flow W (lb/cycle) Measured	Charge-flow error (percent) (a)
0.06	100	8.0	1.903×10^{-3}	1.795×10^{-3}	6.0
.07			1.773	1.748	1.4
.08			2.347	2.376	1.2
.09			2.855	2.863	.3
.10			3.457	3.087	12.0
.11			(b)	(c)	--------
0.06	150	8.0	1.489×10^{-3}	1.526×10^{-3}	2.4
.07			1.407	1.434	1.9
.08			1.815	1.894	4.2
.09			2.310	2.347	1.6
.10			2.911	2.699	7.8
.11			3.611	2.834	27.4
0.06	200	8.0	1.186×10^{-3}	1.187×10^{-3}	0.1
.07			1.110	1.041	6.6
.08			1.459	1.382	5.6
.09			1.813	1.751	3.5
.10			2.301	2.119	8.6
.11			2.894	2.501	15.7
0.06	250	8.0	0.942×10^{-3}	0.996×10^{-3}	5.4
.07			.861	.942	8.6
.08			1.148	1.130	1.6
.09			1.447	1.402	3.2
.10			1.849	1.819	1.6
.11			2.239	2.235	.2
0.06	300	8.0	0.749×10^{-3}	0.820×10^{-3}	8.7
.07			.735	.763	3.7
.08			.933	.871	7.1
.09			1.150	1.126	2.1
.10			1.477	1.481	.3
.11			1.838	1.776	3.5
0.06	350	8.0	0.687×10^{-3}	0.707×10^{-3}	2.8
.07			.679	.663	2.4
.08			.790	.713	10.8
.09			.918	.843	8.9
.10			1.158	1.181	2.0
.11			1.461	1.465	.3

Mean error: 5.1

Variable compression ratio

Fuel-air ratio f	Inlet-air temperature T (°F)	Compression ratio r	Knock-limited charge flow W (lb/cycle) Calculated	Knock-limited charge flow W (lb/cycle) Measured	Charge-flow error (percent) (a)
0.06	250	5.0	2.870×10^{-3}	3.067×10^{-3}	6.4
.07			2.669	2.761	3.5
.08			3.529	3.996	11.7
.09			4.389	5.188	15.4
.10			5.519	5.456	1.2
.11			6.970	(c)	--------
0.06	250	6.0	1.864×10^{-3}	1.731×10^{-3}	7.7
.07			1.767	1.527	15.7
.08			2.292	2.246	2.0
.09			2.895	3.132	7.6
.10			3.619	3.960	8.6
.11			4.571	4.070	12.3
0.06	250	7.3	1.169×10^{-3}	1.258×10^{-3}	7.1
.07			1.076	1.091	1.4
.08			1.448	1.346	7.6
.09			1.780	1.744	2.1
.10			2.268	2.141	5.9
.11			2.838	2.538	11.8
0.06	250	8.7	0.766×10^{-3}	0.855×10^{-3}	10.4
.07			.721	.756	4.6
.08			.936	.900	4.0
.09			1.175	1.148	2.4
.10			1.481	1.467	1.0
.11			1.850	1.746	6.0
0.06	250	10.0	0.558×10^{-3}	0.678×10^{-3}	17.7
.07			.541	.564	4.1
.08			.670	.576	16.3
.09			.804	.741	8.5
.10			1.032	1.005	2.7
.11			1.295	1.332	2.8

Mean error: 7.2

a Error listed without regard for sign.
b Condition not covered by correlation curve.
c No engine data available.

TABLE I – COMPARISON OF CALCULATED AND MEASURED KNOCK-LIMITED CHARGE FLOW IN SUPERCHARGED CFR ENGINE – Concluded

(h) Triptene.

Fuel-air ratio f	Variable inlet-air temperature					Variable compression ratio				
	Inlet-air temperature T_0 (°F)	Compression ratio r	Knock-limited charge flow W (lb/cycle)		Charge-flow error (percent) (a)	Inlet-air temperature T_0 (°F)	Compression ratio r	Knock-limited charge flow W (lb/cycle)		Charge-flow error (percent) (a)
			Calculated	Measured				Calculated	Measured	
0.06	100	8.0	2.558×10^{-3}	2.813×10^{-3}	9.8	250	5.0	3.949×10^{-3}	4.220×10^{-3}	6.4
.07			2.186	2.100	4.1			3.347	3.907	14.3
.08			2.493	2.300	8.4			3.786	4.267	11.3
.09			2.852	2.687	6.1			4.408	4.760	7.4
.10			3.362	3.300	1.9			5.161	5.300	2.5
.11			4.054	4.087	.8			6.417	(b)	-----
0.06	150	8.0	2.067×10^{-3}	2.347×10^{-3}	11.9	250	6.0	2.605×10^{-3}	2.440×10^{-3}	6.8
.07			1.737	1.693	9.0			2.159	2.180	1.0
.08			1.984	1.707	16.2			2.443	2.527	3.3
.09			2.322	2.080	11.6			2.889	3.020	4.3
.10			2.739	2.620	4.5			3.389	3.607	6.0
.11			3.458	3.300	4.8			4.439	4.267	4.0
0.06	200	8.0	1.622×10^{-3}	1.453×10^{-3}	11.6	250	7.3	1.547×10^{-3}	1.433×10^{-3}	8.0
.07			1.335	1.360	1.8			1.297	1.300	.2
.08			1.526	1.493	2.2			1.489	1.453	2.5
.09			1.818	1.807	.6			1.762	1.747	.9
.10			2.138	2.213	3.4			2.105	2.053	2.5
.11			2.775	2.687	3.3			2.704	2.360	14.6
0.06	250	8.0	1.217×10^{-3}	1.240×10^{-3}	1.8	250	8.7	0.987×10^{-3}	0.960×10^{-3}	2.8
.07			1.022	.907	12.7			.863	.773	11.6
.08			1.171	1.073	9.1			.936	.900	4.0
.09			1.390	1.353	2.7			1.118	1.200	6.8
.10			1.665	1.687	1.3			1.356	1.520	10.8
.11			2.153	2.093	2.9			1.714	1.853	7.5
0.06	300	8.0	0.933×10^{-3}	0.953×10^{-3}	2.1	250	10.0	0.647×10^{-3}	0.747×10^{-3}	13.4
.07			.776	.787	1.4			.525	.613	14.4
.08			.905	.835	8.6			.631	.597	5.7
.09			1.048	.993	5.5			.737	.713	3.4
.10			1.287	1.220	5.5			.904	.920	1.7
.11			1.654	1.553	7.9			1.183	1.220	3.0
0.06	350	8.0	0.710×10^{-3}	0.793×10^{-3}	10.5					
.07			.583	.673	13.4					
.08			.679	.707	4.0					
.09			.806	.807	.1					
.10			.982	.947	3.7					
.11			1.277	1.153	10.8					
Mean error					6.0					6.2

a Error listed without regard for sign.
b No engine data available.

TABLE II - COMPARISON OF MEAN ERROR IN KNOCK-LIMITED
CHARGE FLOW CALCULATED USING MEAN $F_3(f)$ WITH
MEAN ERROR IN KNOCK-LIMITED CHARGE FLOW CALCULATED
USING INDIVIDUAL $F_3(f)$

| Fuel | Mean error in calculated knock-limited charge flow (percent) | | | |
| | Variable inlet-air temperature | | Variable compression ratio | |
	Individual $F_3(f)$	Mean $F_3(f)$	Individual $F_3(f)$	Mean $F_3(f)$
28-R	3.5	4.2	4.6	5.5
Aviation alkylate	2.9	6.4	3.9	5.4
S reference	2.7	7.6	3.7	7.0
Diisopropyl	3.7	5.0	4.0	3.9
Triptane	8.6	24.4	6.6	22.4
Cyclopentane	7.3	7.2	7.5	8.6
Cyclohexane	5.1	7.4	7.2	9.0
Triptene	6.0	8.5	6.2	6.6

TABLE III - VARIATION OF FUNCTION OF FUEL-AIR RATIO WITH
CHOICE OF Z FOR DIISOPROPYL AND TRIPTENE

Fuel	Z	Fuel-air ratio, f					
		0.06	0.07	0.08	0.09	0.10	0.11
		Function of fuel-air ratio, $F_3(f)$					
Diisopropyl	3.5×10^{-12}	1.081	1.112	1.000	0.885	0.790	0.690
	6.0	1.070	1.103	1.000	.892	.807	.732
	11.0	1.050	1.083	1.000	.933	.878	.858
Triptene	2.0×10^{-12}	0.976	1.090	1.000	0.862	0.752	0.644
	4.0	.980	1.097	1.000	.899	.793	.675
	6.5	.918	1.115	1.000	.865	.762	.661
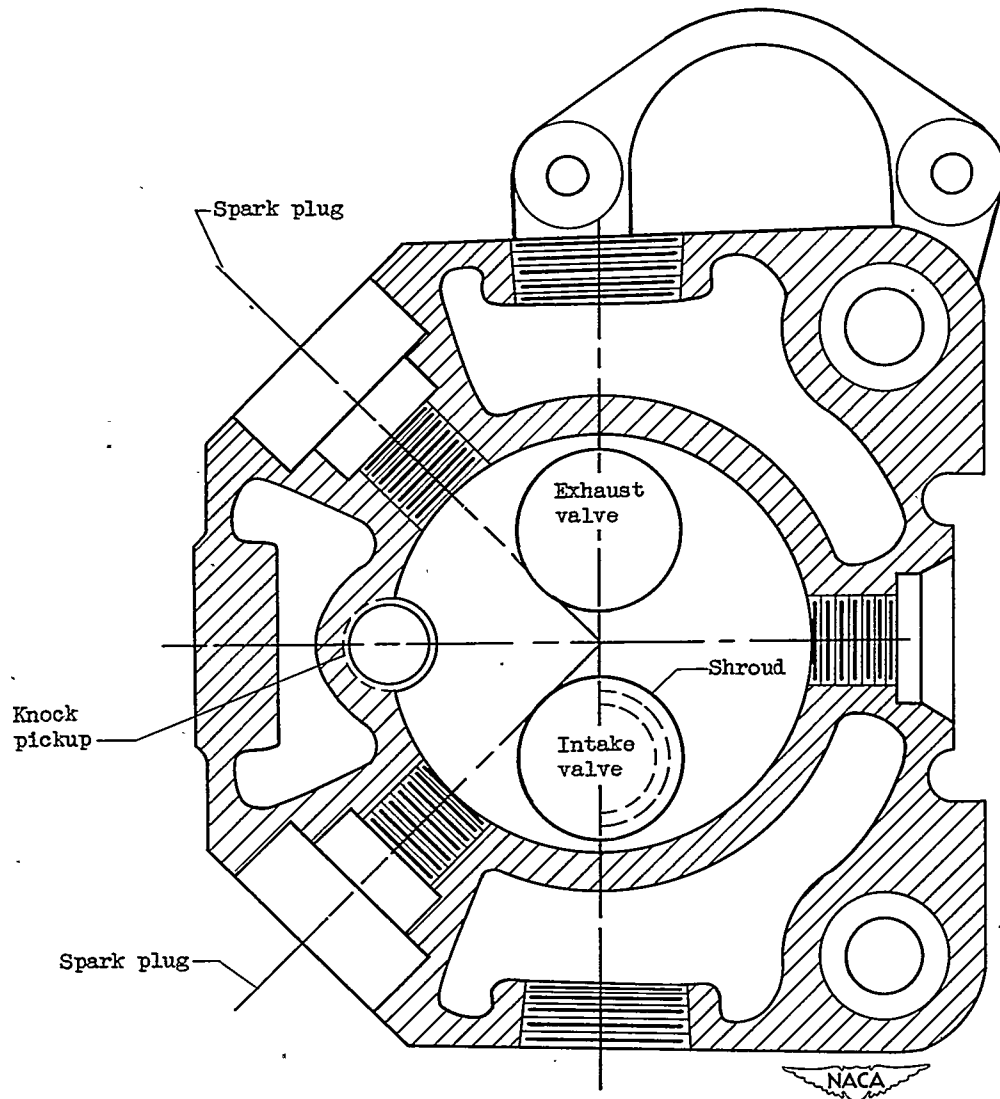
Figure 1. - Schematic diagram of CFR cylinder showing location of spark plugs, knock pick-up, and position of shrouded intake valve.

1225

A   Air-pressure regulator
B   Air supply
C   Thermocouples
D   Air-measuring orifice
E   Air preheater
F   Surge tank

G   Mercury manometer
H   Opening for fuel-injection nozzle
I   Engine cylinder
J   Inlet manifold
K   Differential water manometer
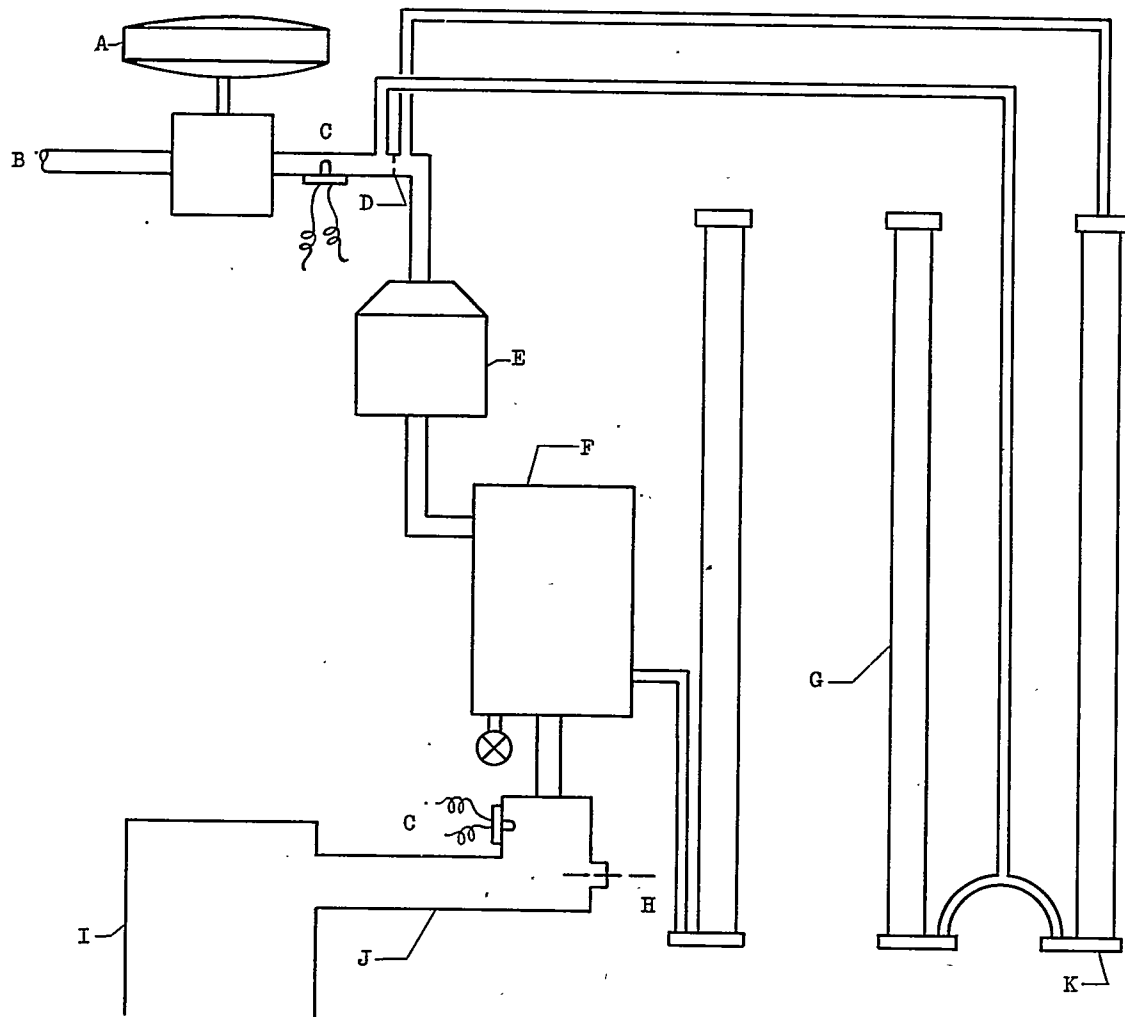
Figure 2. - Schematic diagram of air system.

A Fuel-supply tank   G Pressure-relief valve
B Strainer   H Injection pump
C Solenoid valves   I Pressure gage
D Rotameter   J Fuel cooler
E Fuel-weighing stand   K Circulating pump
F Fuel-injection nozzle
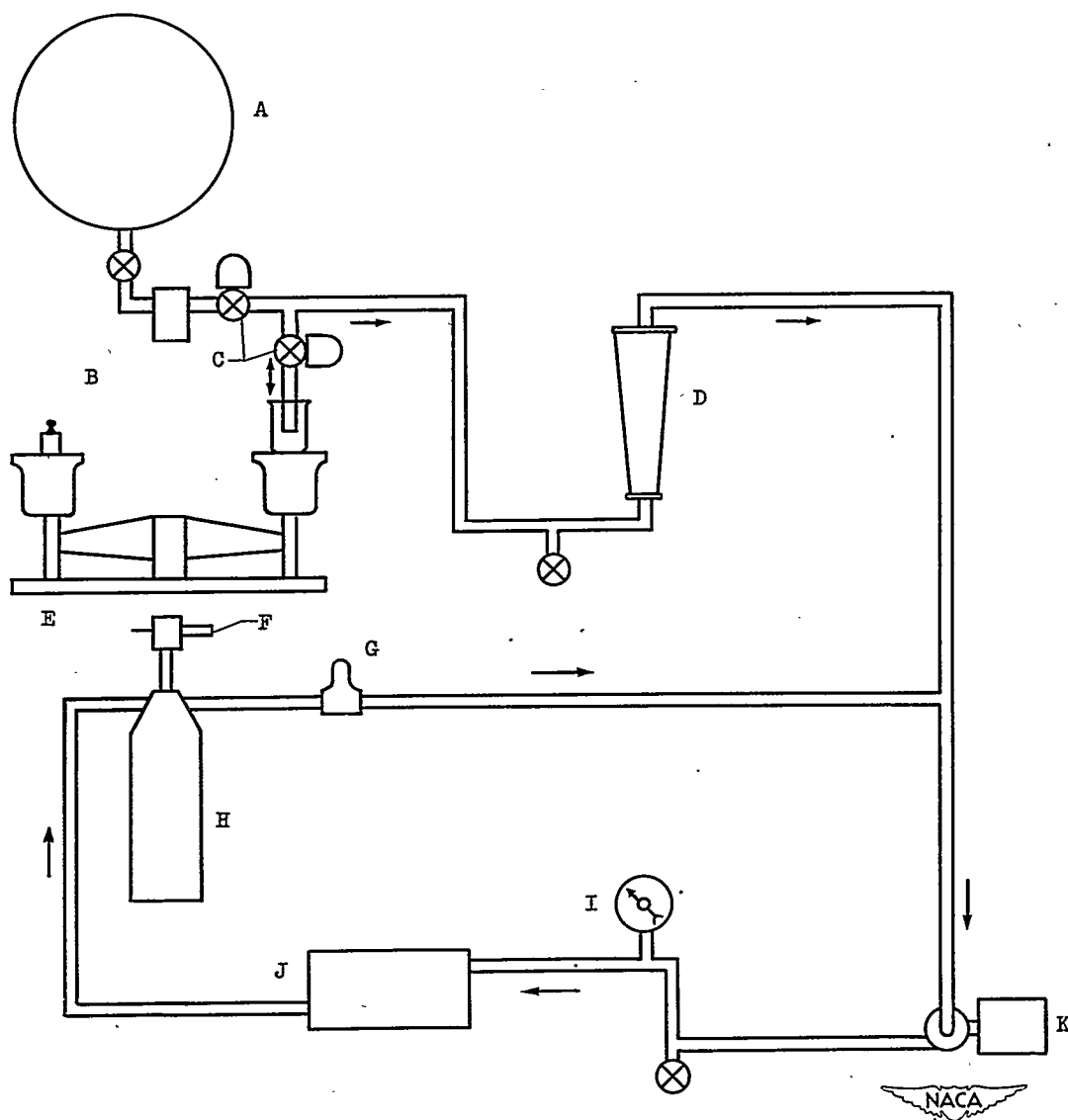
Figure 3. - Schematic diagram of fuel system.
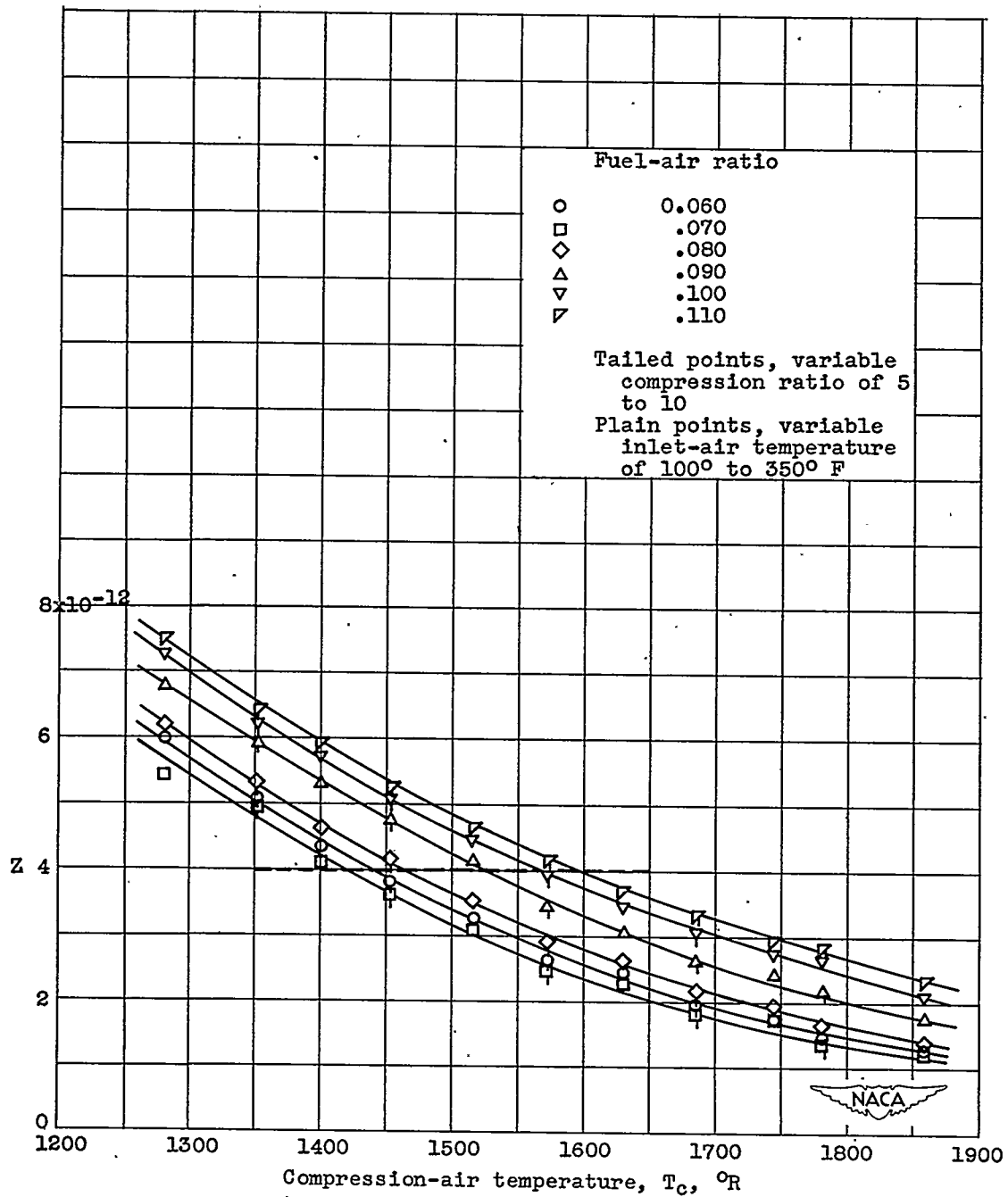
Figure 4. - Effect of compression-air temperature and fuel-air ratio on knock-limited values of Z for 28-R fuel on CFR engine. Data calculated from reference 4. Dashed line indicates value of Z used in computation of function of fuel-air ratio, $F_3(f)$.
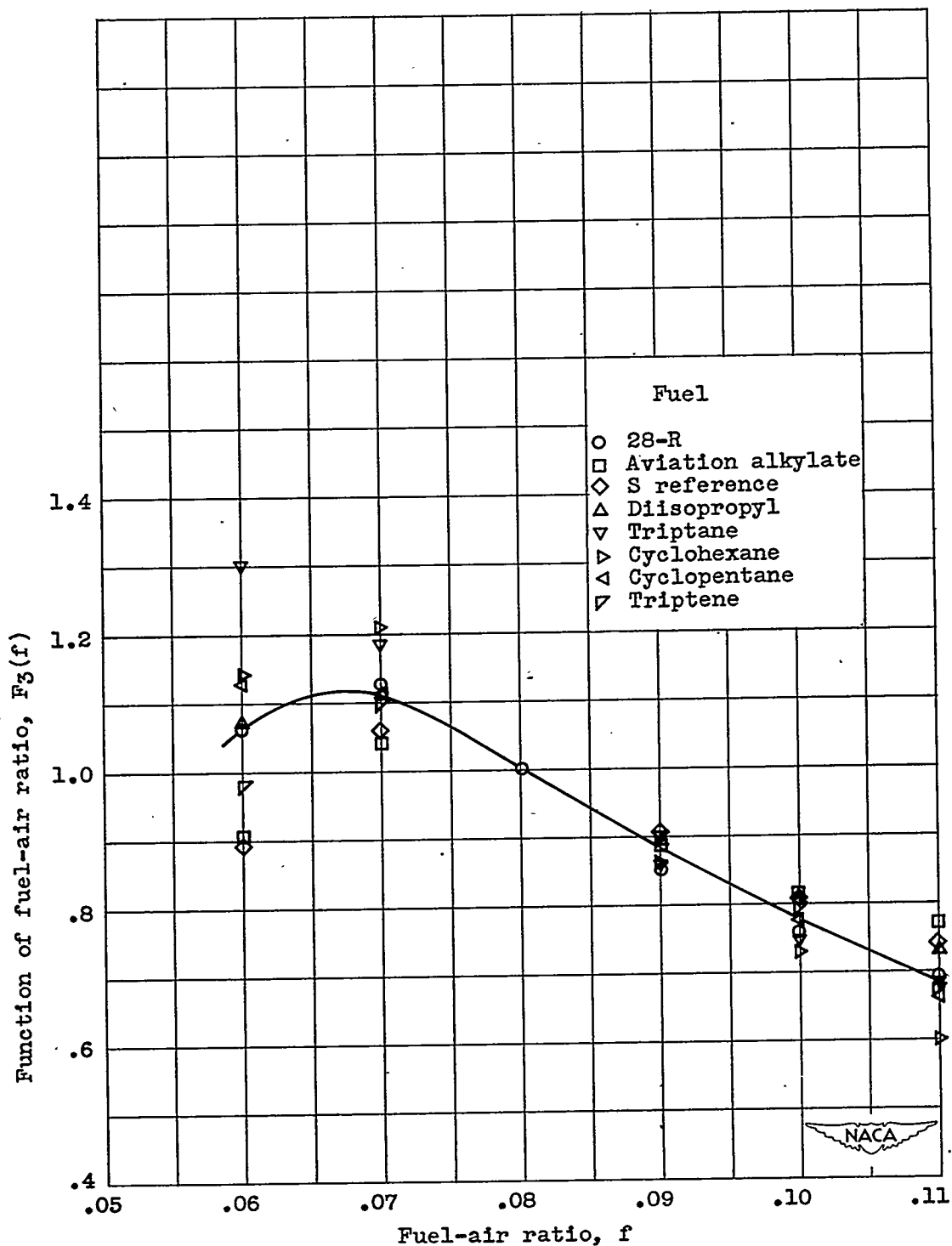
Figure 5. - Effect of fuel-air ratio on function of fuel-air ratio for eight fuels in supercharged CFR engine.
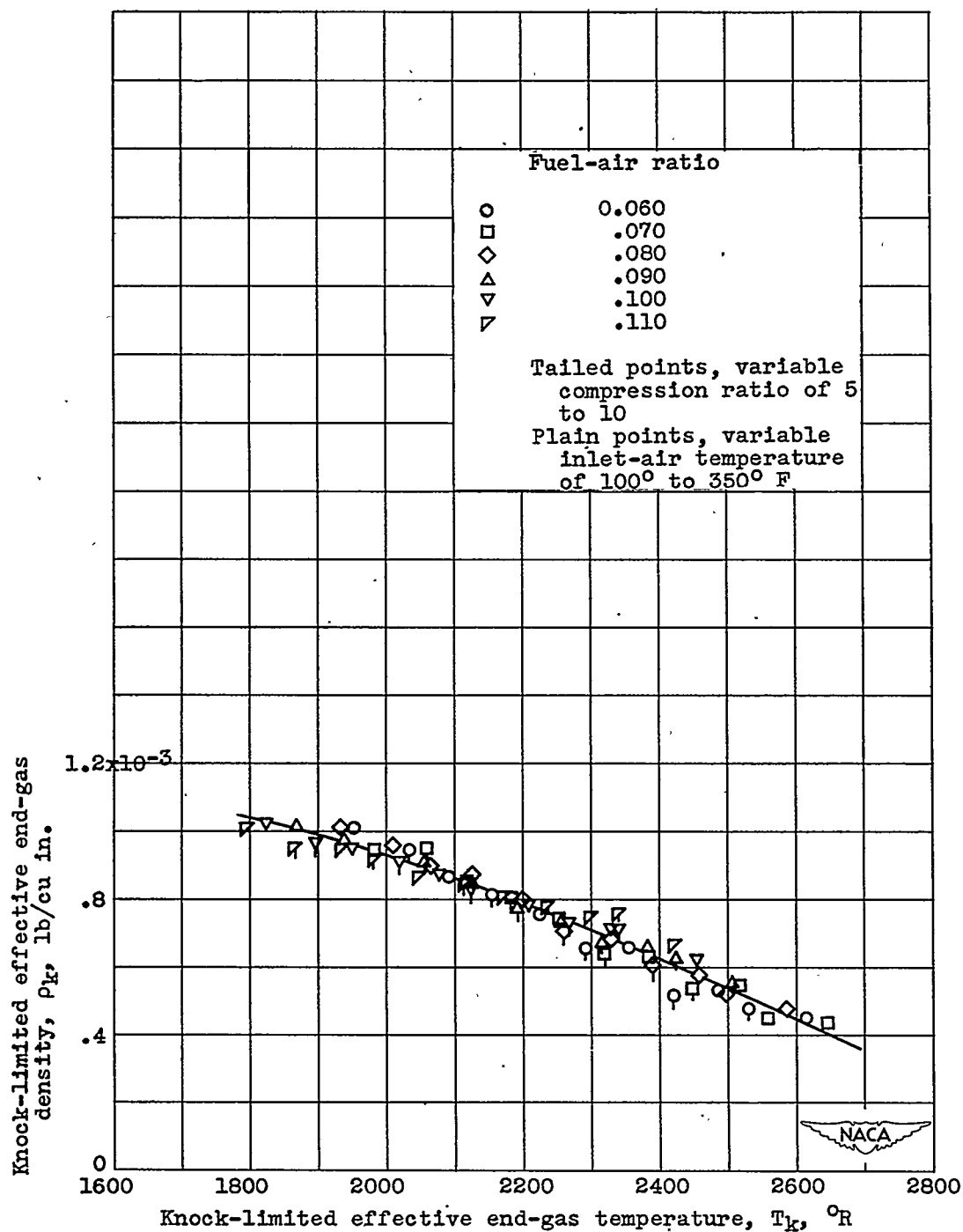
(a) 28-R fuel.

Figure 6. - Variation of knock-limited effective end-gas density with
knock-limited effective end-gas temperature for changes in fuel-air
ratio, inlet-air temperature, and compression ratio. Inlet-air
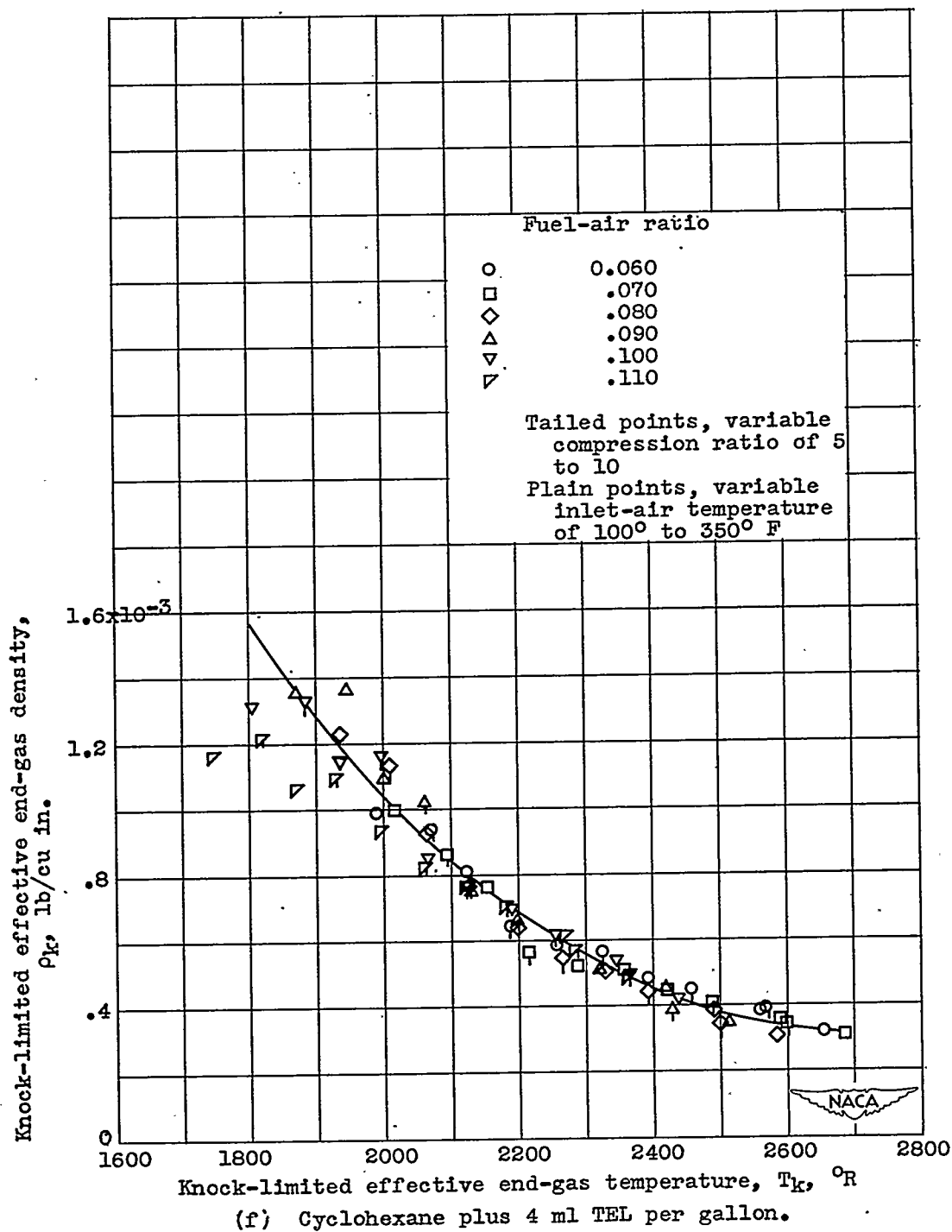pressure varied to maintain incipient knock. (Data calculated from
reference 5.)

Knock-limited effective end-gas temperature, T_k, °R
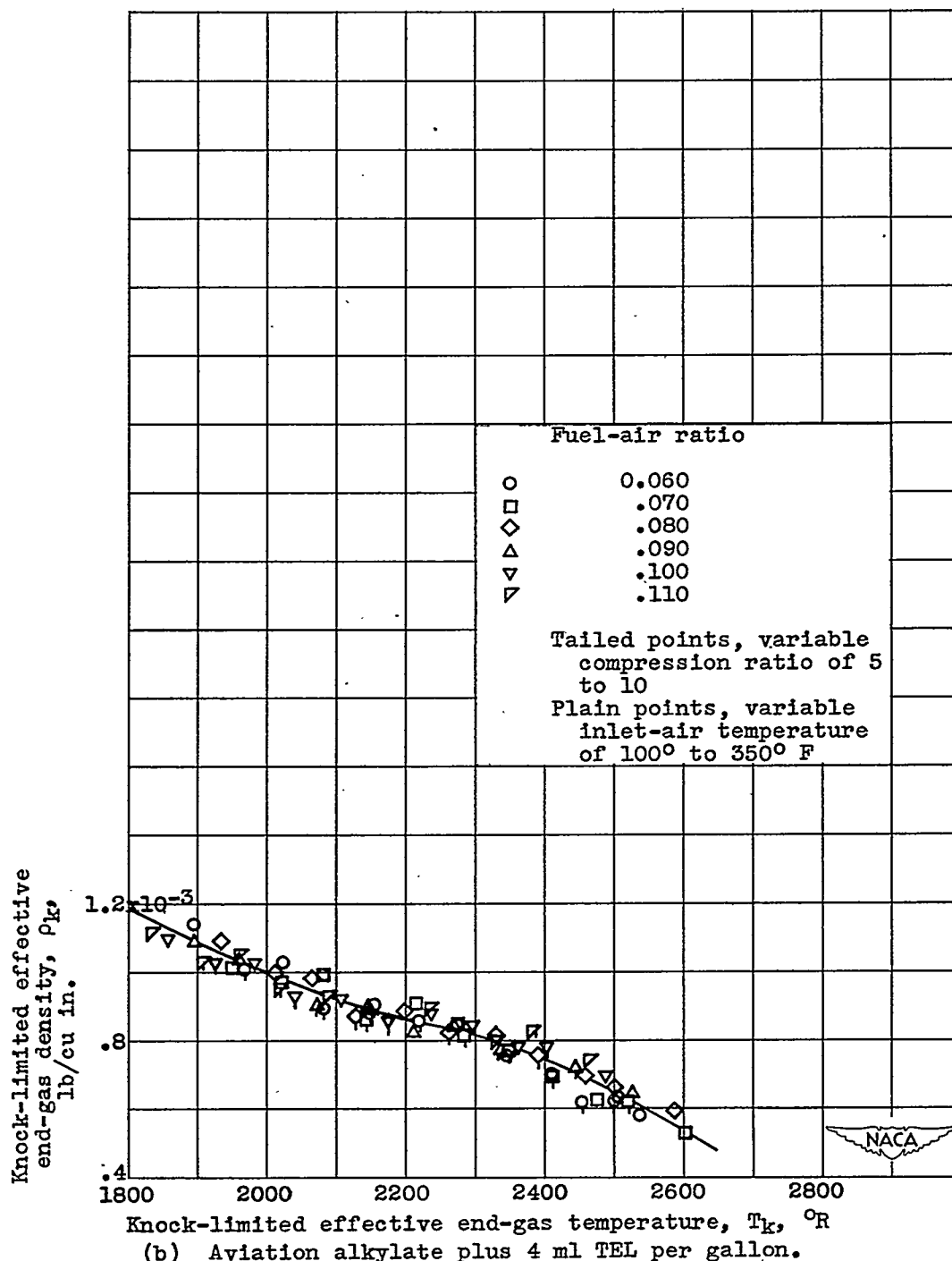
(b)   Aviation alkylate plus 4 ml TEL per gallon.
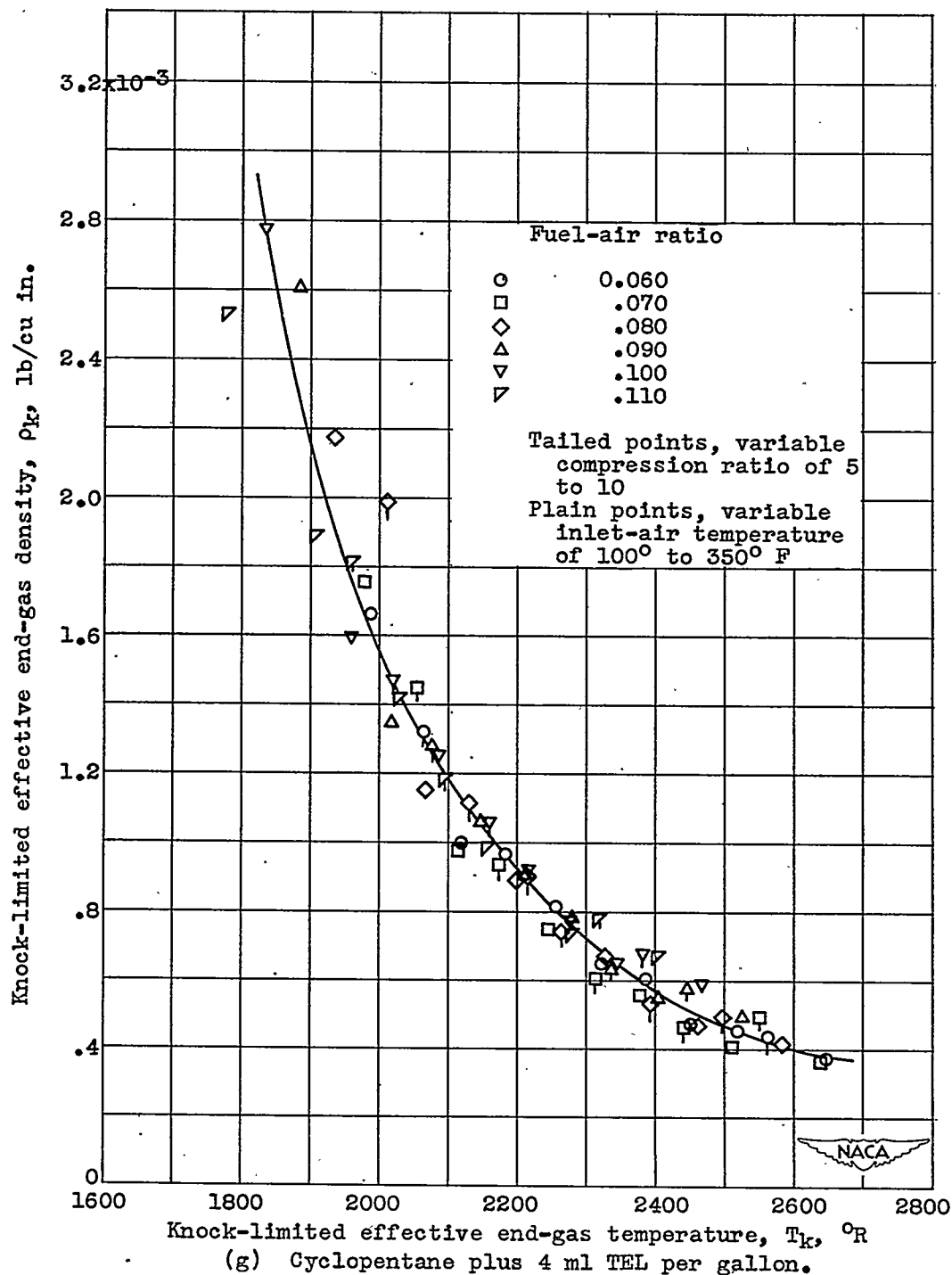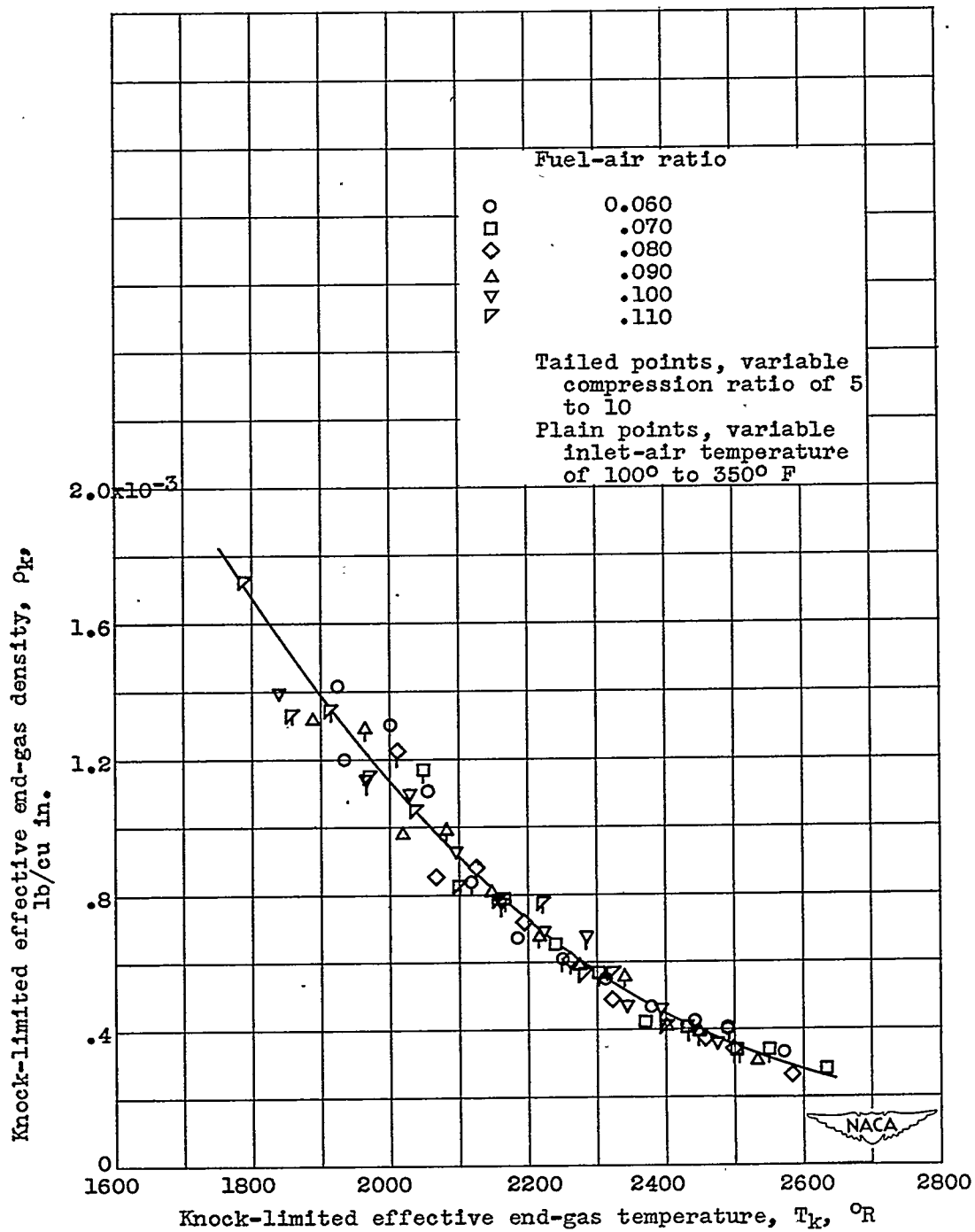
Figure 6. - Continued. Variation of knock-limited effective end-gas
   density with knock-limited effective end-gas temperature for changes
   in fuel-air ratio, inlet-air temperature, and compression ratio. Inlet-
   air pressure varied to maintain incipient knock. (Data calculated
   from reference 5.)

Fuel-air ratio

☉	0.060
□	.070
◇	.080
△	.090
▽	.100
▷	.110

Tailed points, variable
  compression ratio of 5
  to 10
Plain points, variable
  inlet-air temperature
  of 100° to 350° F

Knock-limited effective end-gas density, ρ_k, lb/cu in.

1.6×10^{-3}

1.2

.8

.4

1600   1800   2000   2200   2400   2600   2800

Knock-limited effective end-gas temperature, T_k, °R

(c) S reference fuel plus 4 ml TEL per gallon.

Figure 6. - Continued. Variation of knock-limited effective end-gas
  density with knock-limited effective end-gas temperature for changes
  in fuel-air ratio, inlet-air temperature, and compression ratio.
  Inlet-air pressure varied to maintain incipient knock. (Data
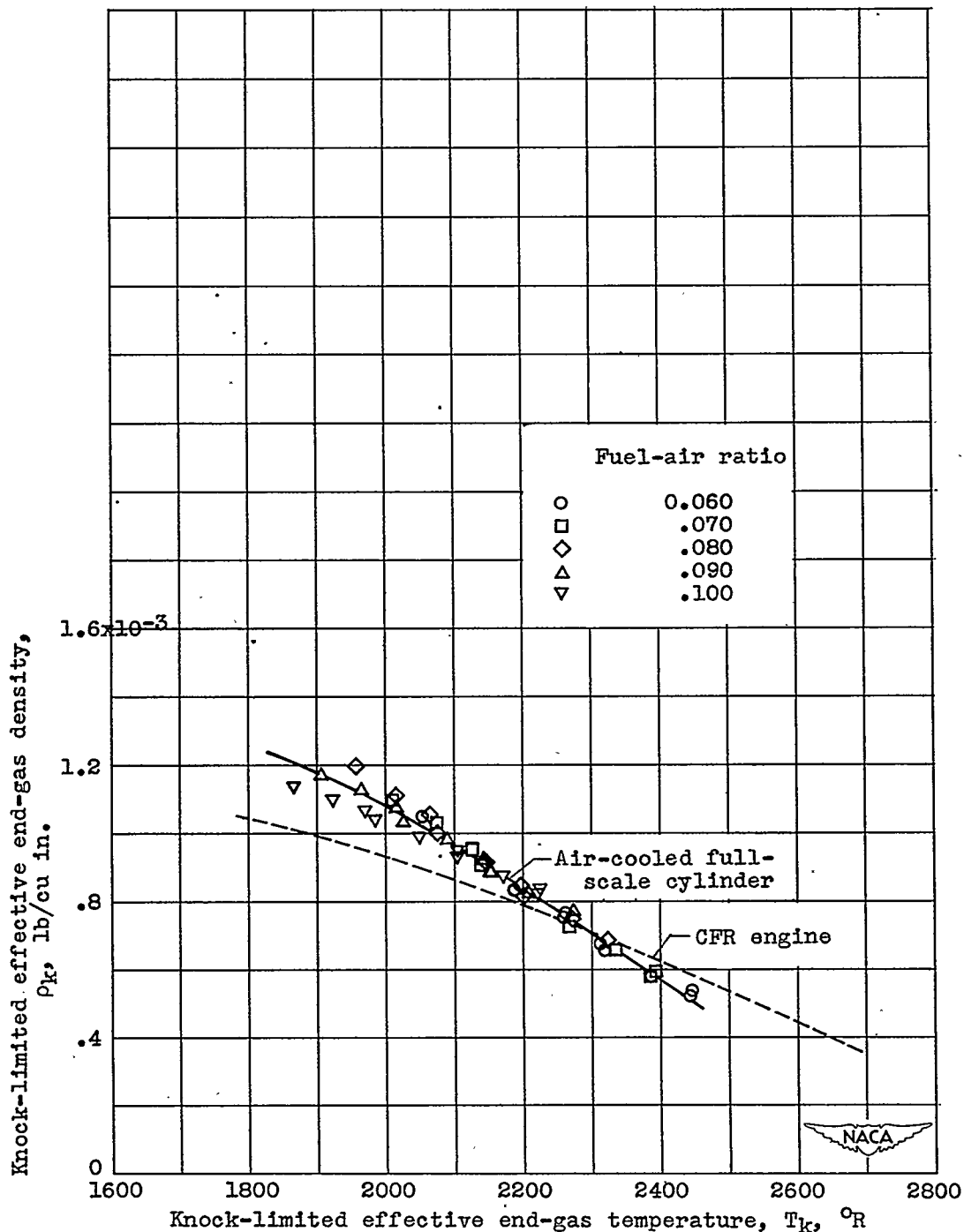 calculated from reference 5.)

(d) Diisopropyl plus 4 ml TEL per gallon.

Figure 6. - Continued. Variation of knock-limited effective end-gas
   density with knock-limited effective end-gas temperature for changes
   in fuel-air ratio, inlet-air temperature, and compression ratio.
   Inlet-air pressure varied to maintain incipient knock. (Data
   calculated from reference 5.)

(e)   Triptane plus 4 ml TEL per gallon.

Figure 6. - Continued. Variation of knock-limited effective end-gas
   density with knock-limited effective end-gas temperature for changes
   in fuel-air ratio, inlet-air temperature, and compression ratio.
   Inlet-air pressure varied to maintain incipient knock. (Data
   calculated from reference 5.)

(f) Cyclohexane plus 4 ml TEL per gallon.

Figure 6. - Continued. Variation of knock-limited effective end-gas
density with knock-limited effective end-gas temperature for changes
in fuel-air ratio, inlet-air temperature, and compression ratio.
Inlet-air pressure varied to maintain incipient knock. (Data
calculated from reference 5.)

1225

(g) Cyclopentane plus 4 ml TEL per gallon.

Figure 6. - Continued. Variation of knock-limited effective end-gas
    density with knock-limited effective end-gas temperature for changes
    in fuel-air ratio, inlet-air temperature, and compression ratio.
    Inlet-air pressure varied to maintain incipient knock. (Data
    calculated from reference 5.)

(h) Triptene plus 4 ml TEL per gallon.

Figure 6. - Concluded. Variation of knock-limited effective end-gas
    density with knock-limited effective end-gas temperature for changes
    in fuel-air ratio, inlet-air temperature, and compression ratio.
    Inlet-air pressure varied to maintain incipient knock. (Data
    calculated from reference 5.)

Figure 7. - Comparison of variation of knock-limited effective end-gas
density with knock-limited effective end-gas temperature for full-
scale cylinder and CFR engine using 28-R fuel. Data obtained for
full-scale cylinder at compression ratio of 6.7 to 8.0 and inlet-air
temperature of 150° to 300° F. Curve for CFR engine plotted from
figure 6(a). Inlet-air pressure varied to maintain incipient knock.
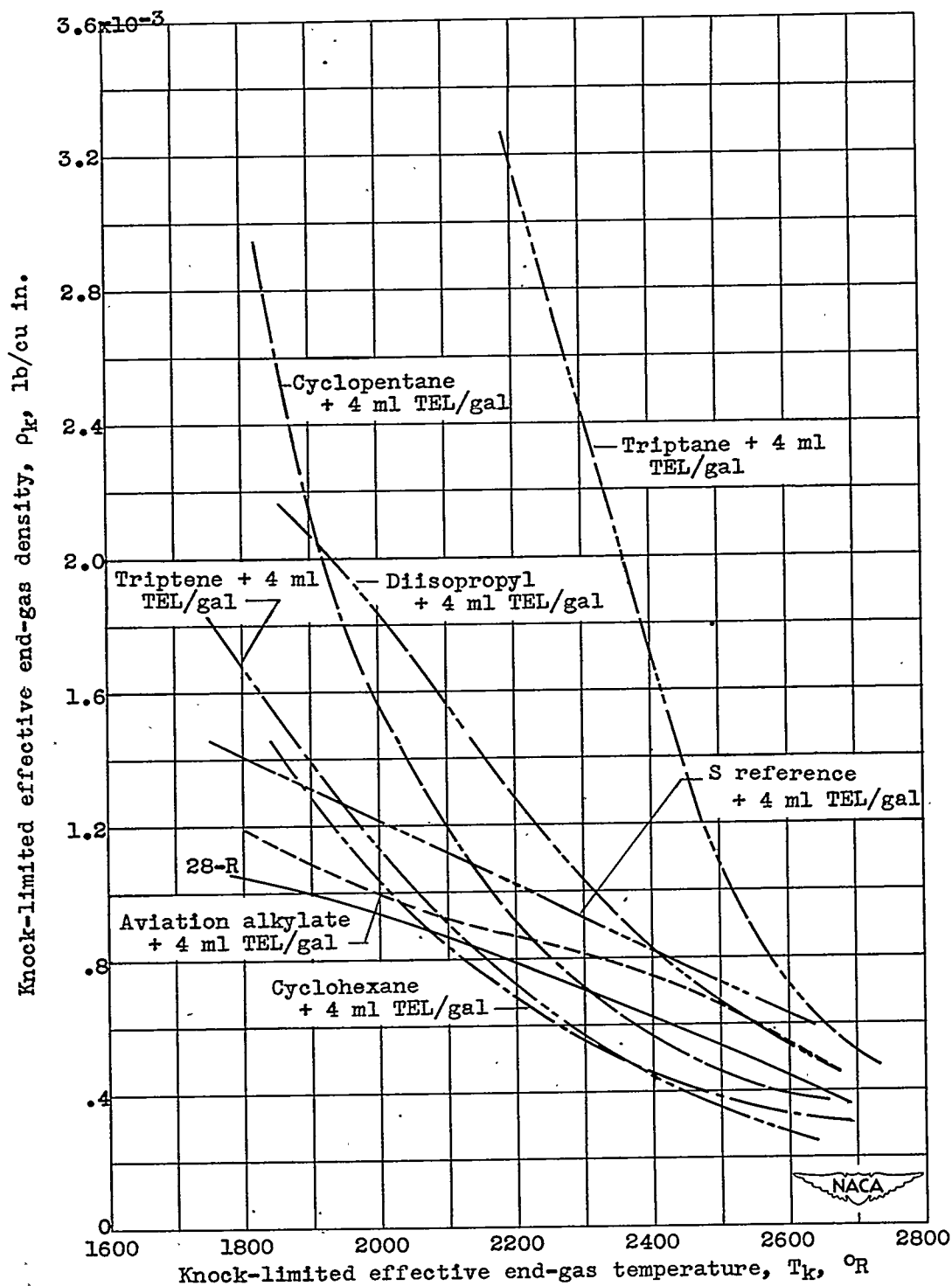
Figure 8. - Superposition of faired curves from figure 6 showing effect of change in knock-limited effective end-gas temperature on knock-limited effective end-gas density for eight fuels.
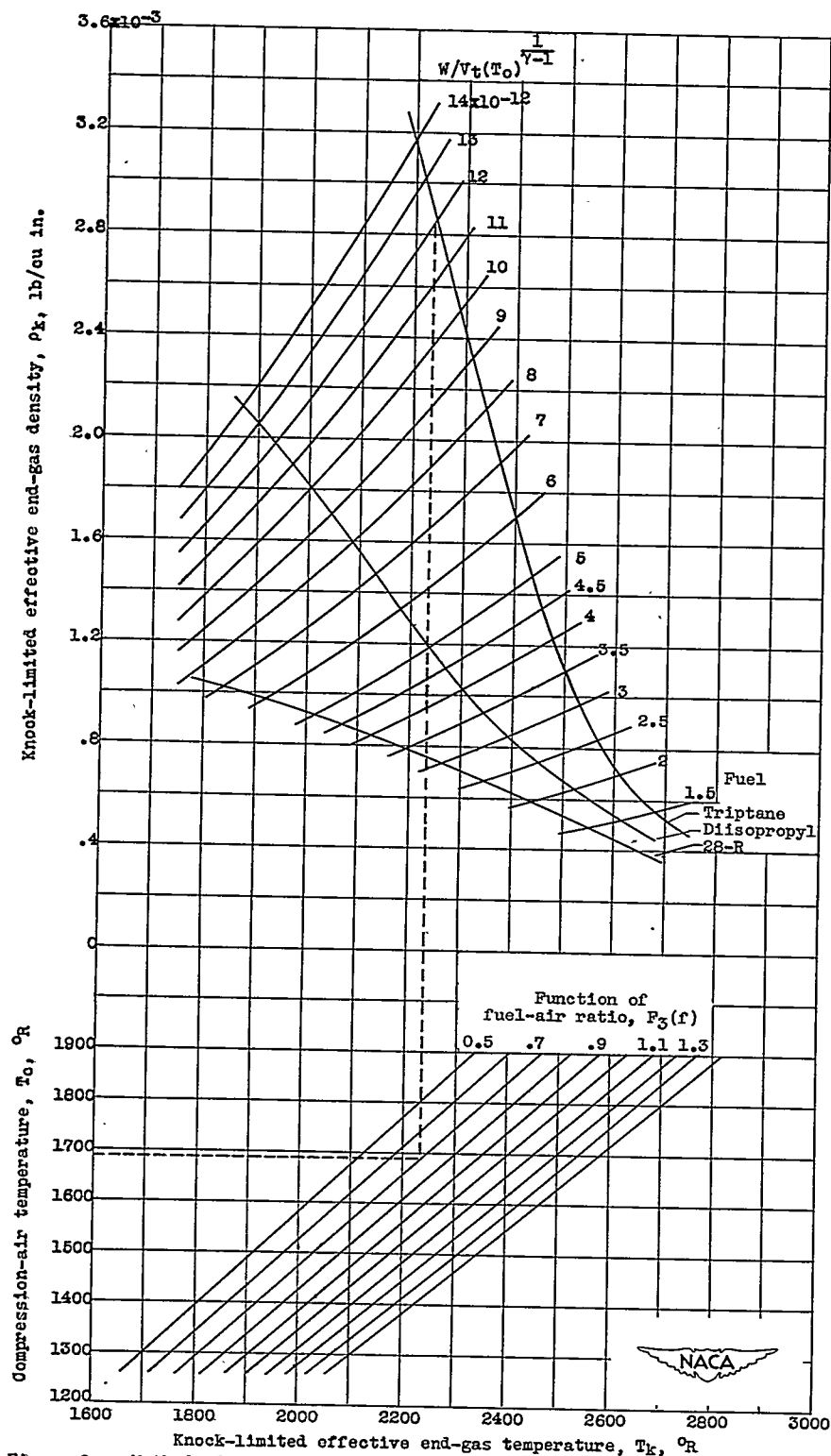
Figure 9. — Method of comparing knock-limited charge flow at fixed inlet conditions for fuels whose curves of knock-limited effective end-gas density plotted against knock-limited effective end-gas temperature are known. Dotted line represents use of chart to obtain value of W for three fuels at inlet-air temperature of 250° F., compression ratio of 8.7, and fuel-air ratio of 0.11. (Curves plotted from figs. 6(a), 6(d), and 6(e).)
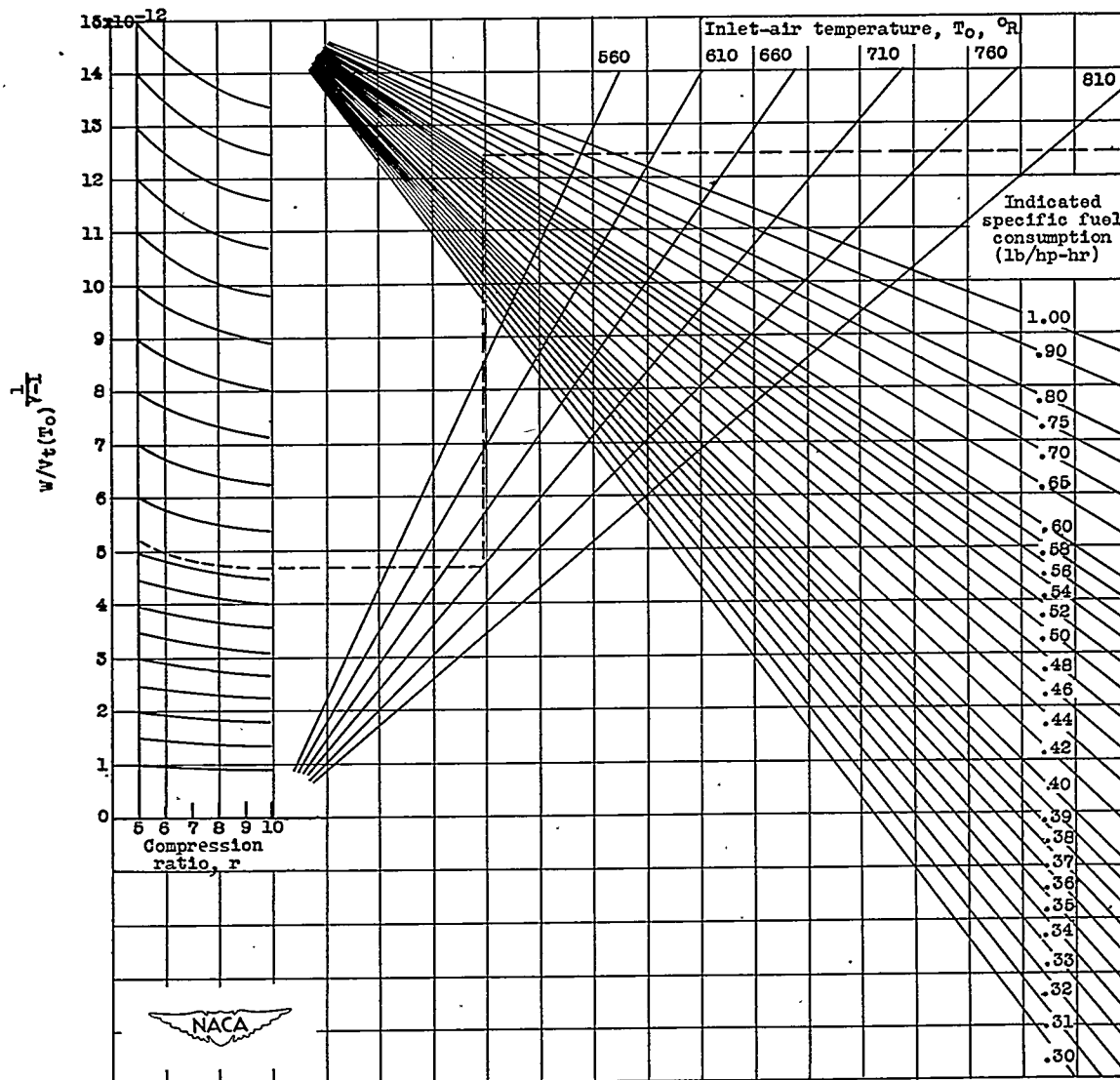
Figure 10. — Chart for calculating indicated mean effective pressure from

1225

Indicated mean effective pressure, imep, lb/sq in. absolute

Fuel-air ratio

0.11
.10
.09
.08
.07
.06
.05

NACA
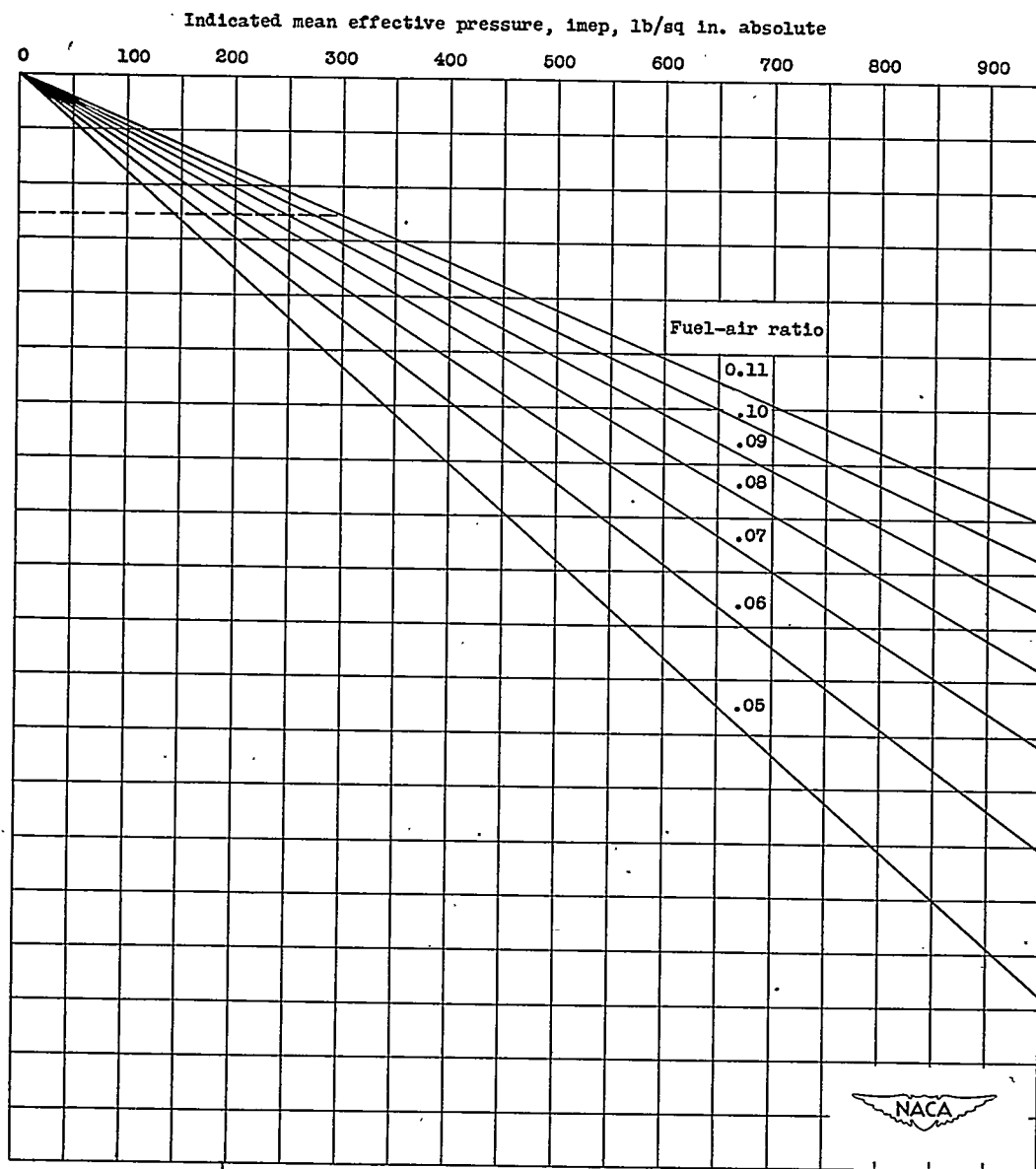
value of $W/V_t(T_o)^{\frac{1}{\gamma-1}}$ determined from figure 9 for any desired inlet conditions.
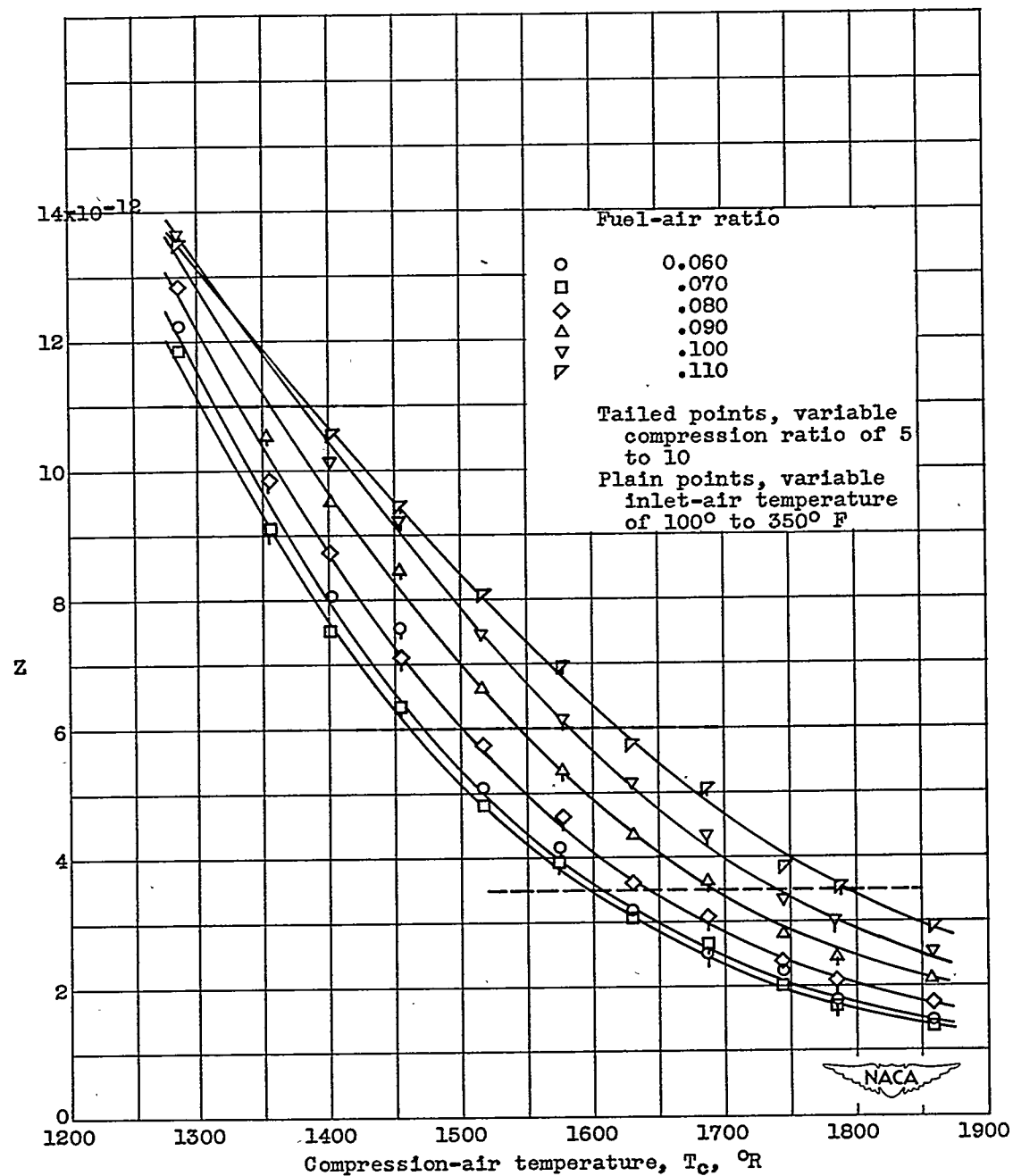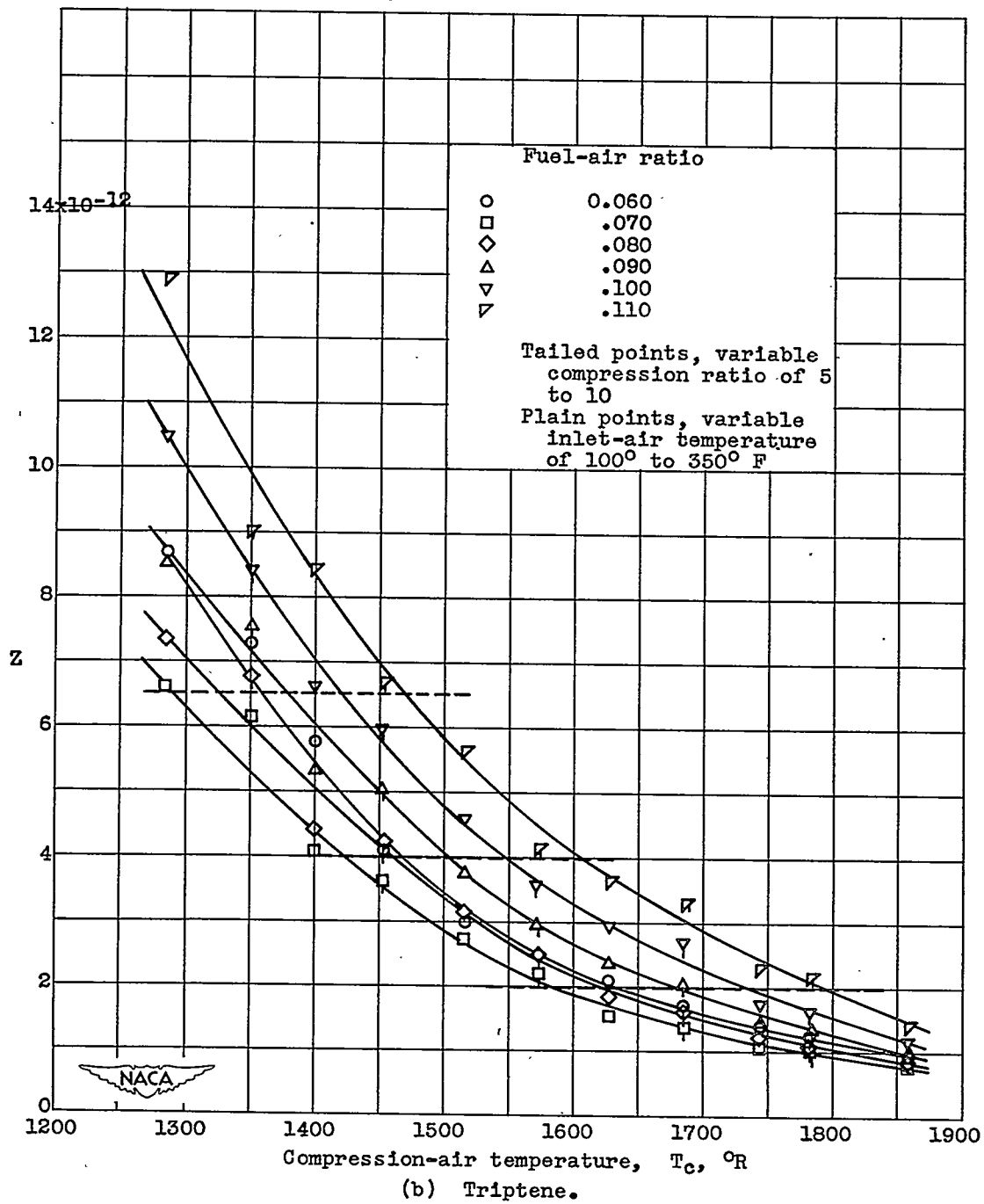
(a) Diisopropyl.

Figure 11. - Variation of Z with compression-air temperature and fuel-air ratio. Dashed lines indicate three values of Z used to compute fuel-air ratios for demonstrating the effect of choice of Z on correlation. (Data calculated from reference 5.)

1225

(b) Triptene.

Figure 11. - Concluded. Variation of Z with compression-air temperature and fuel-air ratio. Dashed lines indicate three values of Z used to compute fuel-air ratios for demonstrating the effect of choice of Z on correlation. (Data calculated from reference 5.)
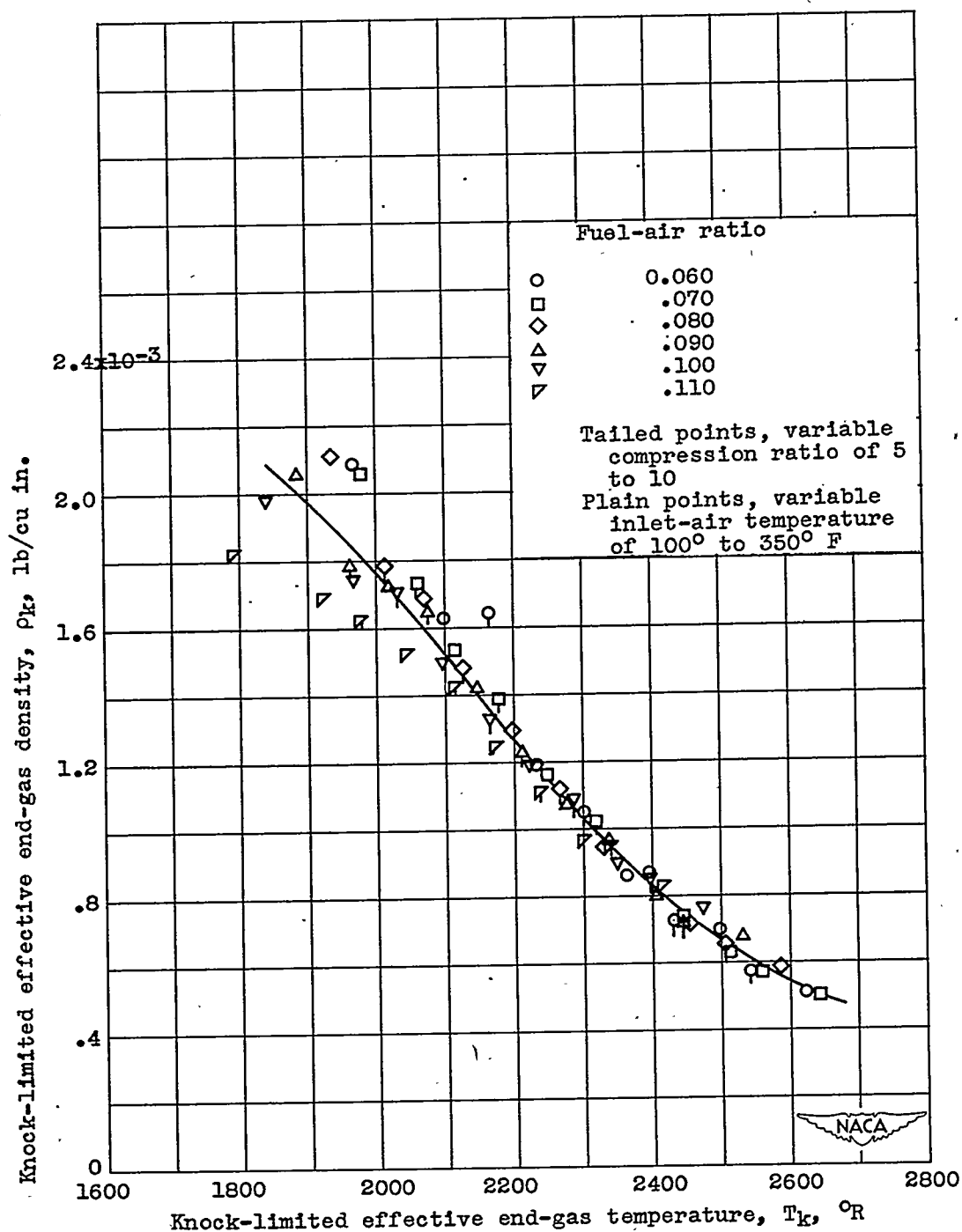
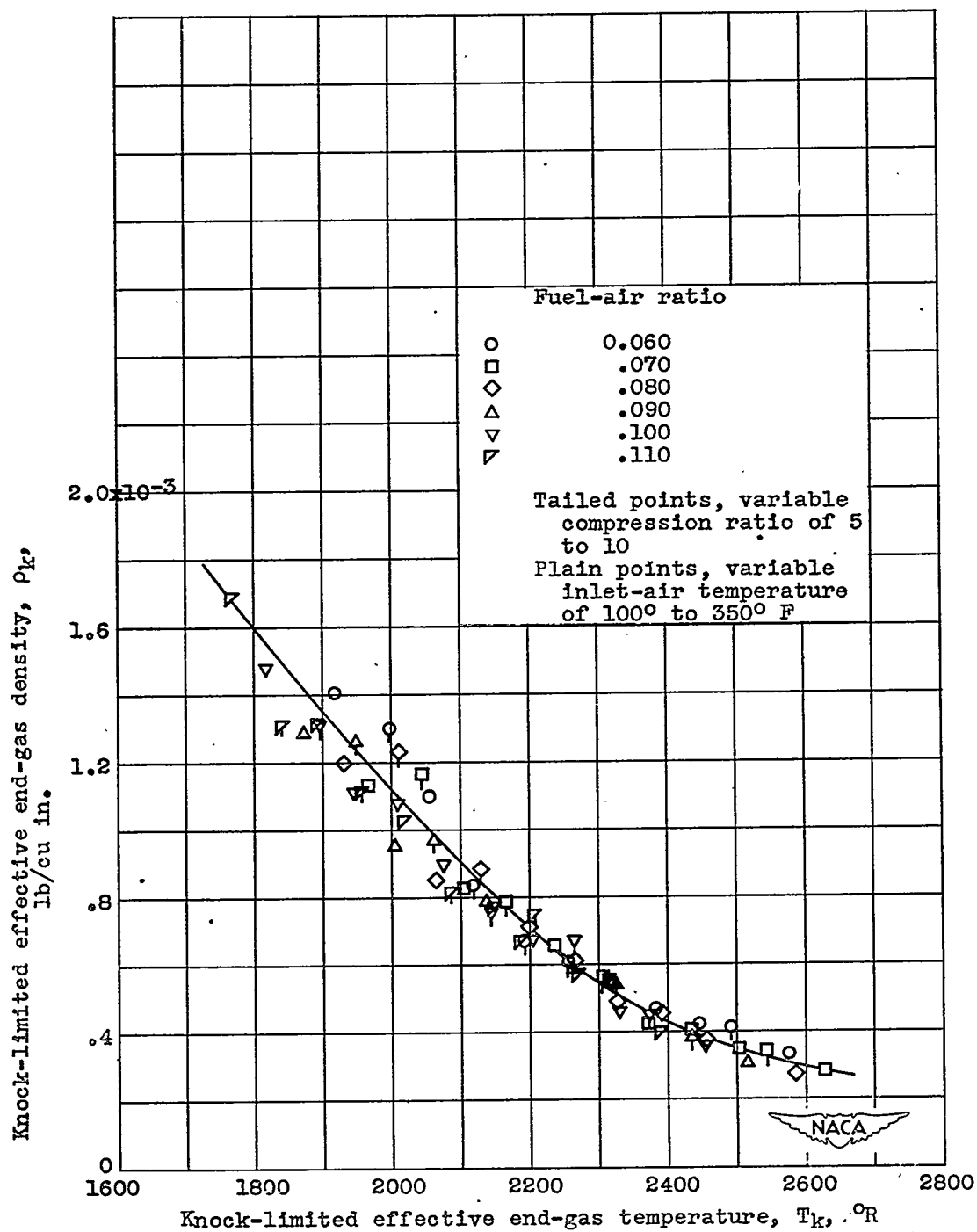(a) Function of fuel-air ratio computed at $Z = 3.5 \times 10^{-12}$.

Figure 12. - Effect of choice of Z on variation of knock-limited effective end-gas density with knock-limited effective end-gas temperature for changes in fuel-air ratio, inlet-air temperature, and compression ratio for diisopropyl plus 4 ml TEL per gallon. Inlet-air pressure varied to maintain incipient knock. (Data calculated from reference 5.)
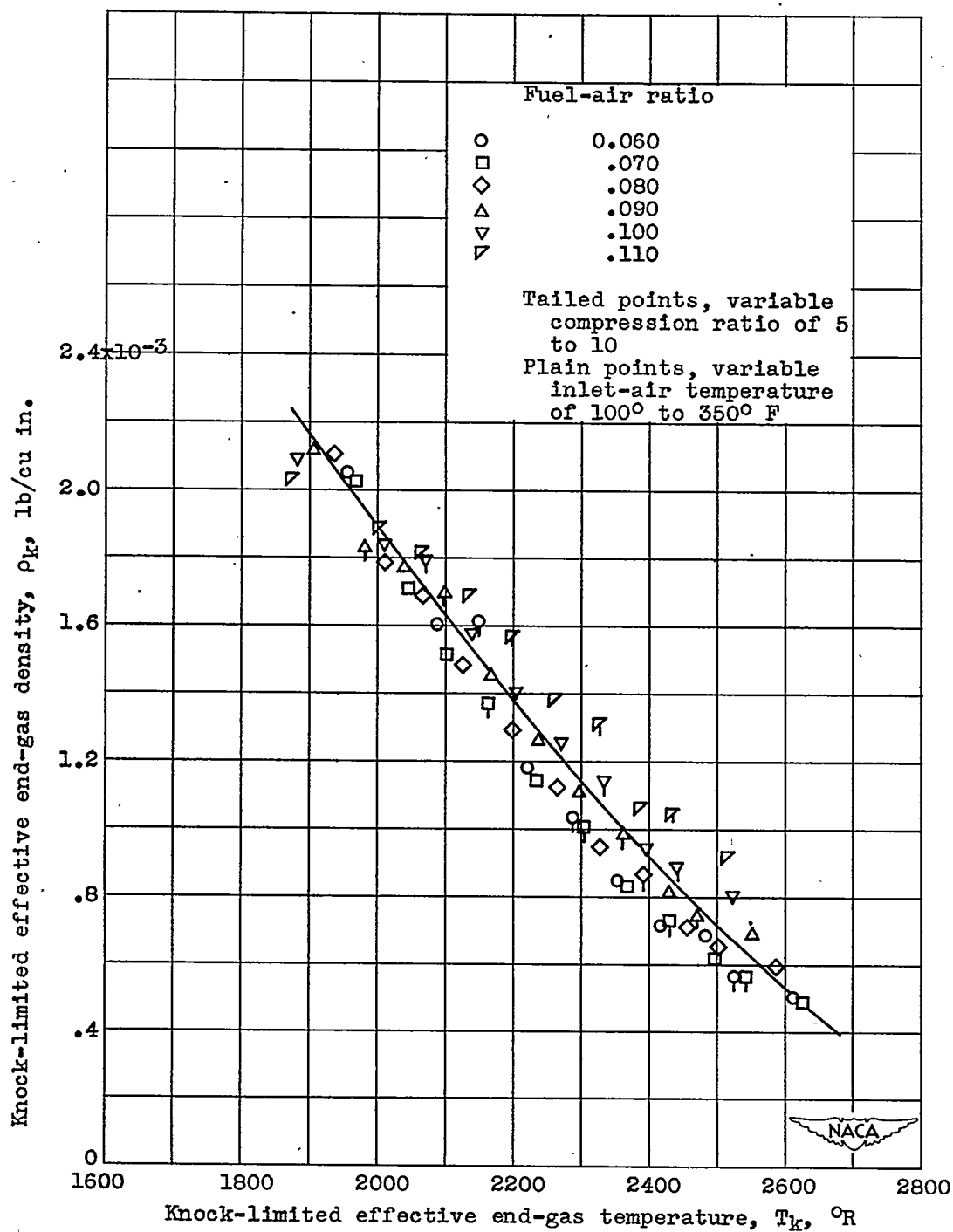
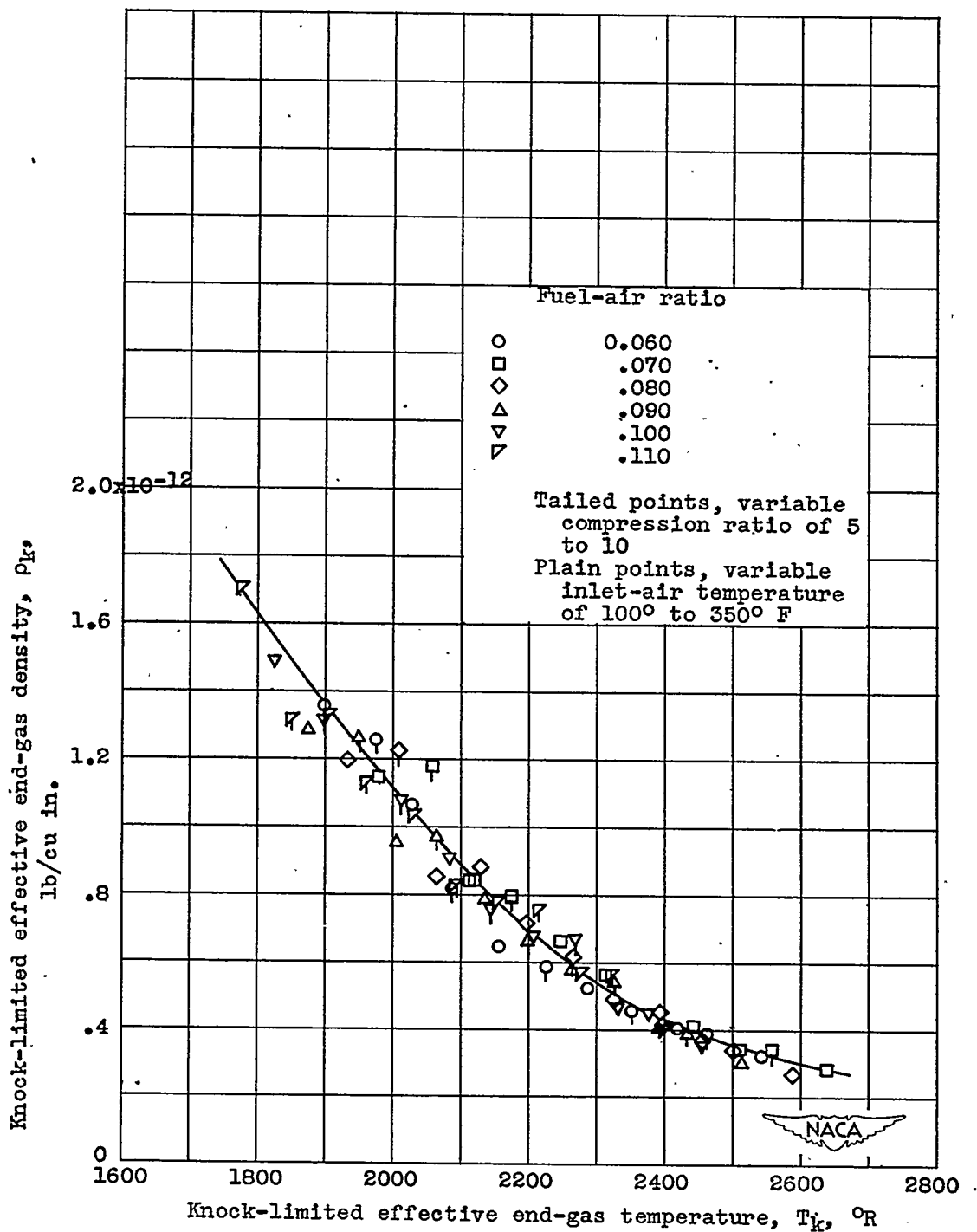(b) Function of fuel-air ratio computed at Z = 11 x 10⁻¹².

Figure 12. - Concluded. Effect of choice of Z on variation of
  knock-limited effective end-gas density with knock-limited effective
  end-gas temperature for changes in fuel-air ratio, inlet-air temper-
  ature, and compression ratio for diisopropyl plus 4 ml TEL per gallon.
  Inlet-air pressure varied to maintain incipient knock. (Data
  calculated from reference 5.)

(a)   Function of fuel-air ratio computed at $Z = 2.0 \times 10^{-12}$.

Figure 13. - Effect of choice of Z on variation of knock-limited
effective end-gas density with knock-limited effective end-gas
temperature for changes in fuel-air ratio, inlet-air temperature,
and compression ratio for triptene plus 4 ml TEL per gallon.
Inlet-air pressure varied to maintain incipient knock.   (Data
calculated from reference 5.)

(b) Function of fuel-air ratio computed at Z = 6.5 x 10^{-12}.

Figure 13. - Concluded. Effect of choice of Z on variation of knock-limited effective end-gas density with knock-limited effective end-gas temperature for changes in fuel-air ratio, inlet-air temperature, and compression ratio for triptene plus 4 ml TEL per gallon. Inlet-air pressure varied to maintain incipient knock. (Data calculated from reference 5.)